Molecules & morphology reveal 'new' divergent, widespread Lampsiline species (Bivalvia: Unionidae)

A THESIS SUBMITTED TO THE FACULTY OF THE GRADUATE SCHOOL OF THE UNIVERSITY OF MINNESOTA

BY

Sean Michael Keogh

IN PARTIAL FULFILLMENT OF THE REQUIREMENTS FOR THE DEGREE OF MASTER OF SCIENCE

Andrew M. Simons

June 2018

Table of Contents

List of Tables

List of Figures

INTRODUCTION

Historically, biodiversity has been recognized almost exclusively by morphological diagnosability. This unidimensional approach has impaired our ability to recognize cryptic diversity. Cryptic diversity is particularly problematic in freshwater mollusks where conchological features traditionally used for species descriptions can be extremely conserved, or alternatively, plastic due to development, sex, and environment. In some cases, this problem can be alleviated by delimiting species using molecular or ecological characters. These additional sources of data and tools to analyze these data such as molecular phylogenetics and ecological niche modeling have fundamentally altered our ability to recognize biodiversity (Fujita *et al.* 2012; Carstens *et al.* 2013). Additionally, definitions of biodiversity have become more inclusive with modern species concepts such as the generalized lineage concept used herein, which defines species as separately evolving metapopulation lineages with no requirement that species possess unique morphological characters (De Queiroz 2007).

Phylogeographic analyses of freshwater mollusks have repeatedly revealed divergent cryptic lineages (Hershler *et al.* 2013; Inoue *et al.* 2018; Kuehnl 2009; Pfenninger *et al.* 2003; Pfeiffer *et al.* 2016; Pieri *et al.* 2018; Smith *et al.* 2018). Most studies have found that cryptic diversity corresponded to allopatric distributions in unique biogeographic regions but some studies have identified cryptic taxa living in sympatry (Hershler *et al.* 2013; Pieri *et al.* 2018). Conversely, freshwater mollusk phylogeographic research has also revealed an overestimation of diversity in some cases (Inoue *et al*. 2013; Inoue *et al*. 2018; Pfeiffer *et al*. 2018; Buhay *et al*. 2002; Mulvey *et al.* 1997). These two alternative findings are not surprising given the high intraspecific phenotypic

plasticity shown in some mollusk taxa and the phenotypic stasis exhibited across others. However, these findings do emphasize the massive problem of morphology-driven species delimitation in biodiversity research and more specifically in freshwater mollusks.

The freshwater mollusk family Unionidae represents the greatest radiation of freshwater bivalves on earth. Unionids have received increasing attention as they are considered one of the most imperiled groups of organisms in North America and because of their fascinating life histories that depend on parasitizing other aquatic animals, typically fishes. In the unionid genus *Lampsilis* (Tribe Lampsilini), all endemic to North America, 26% of 23 extant species are federally listed as threatened or endangered by the U.S. Fish & Wildlife Service and one species, *Lampsilis binominata*, has gone extinct in the last half century (Haag & Williams 2014). *Lampsilis* species are well known for their sophisticated host attraction strategies, with females utilizing a portion of their mantle for mimicry of host prey items (Haag 2012).

One member of the genus, *Lampsilis teres*, has a wide distribution and a high degree conchological variation. *Lampsilis teres* is distributed across several biogeographic regions, (as defined by Haag 2010), including throughout the Upper & Lower Mississippi, Ohio, Tennessee-Cumberland, Interior Highlands, Great Plains, Mobile Basin, Pearl-Pascagoula, Sabine-Trinity, and Western Gulf regions (Haag 2012). Populations in the southern extent of the distribution of *L. teres*, in the isolated Eastern Gulf region were recently elevated to a species status as *Lampsilis floridensis*, based on unpublished conchological and genetic differences (Williams *et al*. 2008). Additionally, even excluding *L. floridensis*, *L. teres* is widely recognized as morphologically variable

(Watters *et al.* 2009; Parmalee & Bogan 1998; Williams *et al.* 2008) and morphological variants have been sporadically recognized as subspecies or distinct species (Rafinesque 1820; Lea 1831; Smith 1899).

A confusing array of names exists for these forms and the correct attribution of these names is not clear. *Lampsilis teres* was originally described by Rafinesque in 1820 with no diagram and abstract shell measurements. *Lampsilis anodontoides* was described by Lea in 1831 with a diagram and shell measurements that closely resembled Rafinesque's *L. teres* description. Lea openly rejected all of Rafinesque's species stating "Mr. R[afinesque]. has, so far from advancing science by his writings in this branch, been the cause of inextricable confusion, from the embarrassment of which we can only be relieved by altogether avoiding any further attempt to make out his imaginary species" (Lea 1852). In 1899, Smith described *Lampsilis fallaciosus = L. fallaciosa* with photographs that again resemble Rafinesque's *L. teres* description as does his type specimen (USNM 30023a) (Figure 1.10). Smith also used Lea's *L. anodontoides* to recognize a specimen with noticeably different shell morphology. A number of authors since have applied these species names seemingly at random to morphological variants of *L. teres*. The proliferation of names and their inconsistent application underscores the taxonomic difficulties posed by this group.

Since Turgeon 1988, *L. teres* has been recognized as a monotypic species with two morphological variants. The more widespread form is cylindrical in shell outline with periostracum coloration varying from bronze to yellow, sometimes with green rays, and is typically smaller in size. For clarity, I will refer to this phenotypic variant as *Lampsilis teres*. The less common form is more circular in shell outline with a thick,

robust shell. Its periostracum is typically uniformly bright yellow, typically lacking green rays (though these are sometimes present on juveniles). I will refer to this form as *Lampsilis anodontoides*. Since Turgeon (1988), these variants are recognized as conspecific, and assumed to be the product of ecophenotypic plasticity (Parmalee & Bogan 1998; Williams *et al.* 2008; Watters *et al.* 2009). However, preliminary examination of museum specimens indicated that morphological variants frequently occurred in sympatry and on multiple occasions were collected syntopically, arguing against an ecophenotypic explanation. In this study, I test the hypothesis that *L. teres* is a single species using several approaches. First, I used molecular data in phylogenetic analyses of *Lampsilis* to determine whether morphological variants of *L. teres* were monophyletic and whether they were each other's closest living relatives. Second, I used morphological data to determine whether morphological variants represented points along a continuum of morphological variation, or whether the variants represented distinct morphologies with useful conchological characters that could be used for diagnosis and field identification. Lastly, when available, I integrated data from species descriptions including quantifiable shell morphology (either reported shell dimensions or diagrams) into my morphological datasets to address the proper taxonomic treatment of diagnosable forms in the *Lampsilis teres* species complex.

MATERIALS & METHODS

Taxon Sampling

I collected 108 specimens of the *Lampsilis teres* complex comprising both morphological groups from 36 locations across the species range (Table 1.1, Figure 1.1). Outgroups *Lampsilis floridensis* Lea (ten individuals), *Lampsilis hydiana* Lea (seven), and *Lampsilis siliquoidea* Barnes (two) were collected from single localities while *Lampsilis straminea* Conrad (three) was collected from three locations. Additional sequences of *Lampsilis* and more distant outgroups were obtained from GenBank.

DNA Extraction, Amplification, Sequencing

For molecular characterization of these samples, I used the protein coding mitochondrial gene *cytochrome c oxidase subunit I* (COI) and the nuclear-encoded ribosomal *internal transcribed spacer I* (ITSI). Total genomic DNA was extracted from the mantle or foot tissue, or from epithelial cells sampled non-lethally using tissue swabs, using the Qiagen DNAeasy Blood and Tissue Kit (Qiagen, Valencia, CA). I used PCR to amplify COI for all but 15 individuals and ITSI for a subset of individuals from each species and morphological group. PCRs were carried out in solution with total volume 12.5 uL, containing 1.5 uL template DNA, 2.75 uL water, 6.25 uL GoTaq Green Master Mix (Promega, Madison, WI), and 1.0 uL of each forward and reverse primer. Primers for PCR amplification of COI were LCO1490 and HCO2198 as described in Folmer *et al.* 1994 using the temperature profile 94 C for 60 s (denaturation), 45 C for 60 s (annealing), 72 C for 90 s (extension) for 35 cycles. COI could not be amplified for 15

museum specimens. Instead I developed primers to amplify an informative ~160 bp region of COI: 436 F (5'-GCT GGT GCT TCT TCT ATT TTG GG-3') and 595 R (5'-TAG CAC CAG CCA AAA CAG GTA-3'). Primers were developed in Geneious v6.1.6 and the PCR temperature profile was the same as COI with exception of an increased annealing temperature of 53 C. Primers used for ITSI were 18s and 5.8s described in King *et al.* 1999 and an identical temperature profile for PCR amplification was used. PCR products were purified using Exonuclease 1 and Shrimp Alkaline Phosphatase (SAP). Purified PCR products were sequenced using ABI BigDye Terminator v3.1 chemistry at the University of Minnesota Genomics Center (UMGC).

Genetic Analysis

Heavy and light strands were assembled into contiguous sequences and aligned using the MUSCLE algorithm in Geneious v6.1.6 (Edgar 2004). The COI alignment was translated into amino acids to confirm the absence of stop codons and determine codon positions. Sequencing of the ITSI locus proved more difficult (some sequences were excluded due to poor quality), however I observed no evidence of polymorphic sites or length polymorphism for included sequences. The COI and ITSI alignments were trimmed to a maximum of 712 and 526 nucleotides respectively. Sequences generated in this study have been submitted to GenBank.

Phylogenetic Analysis

I used PartitionFinder v1.01 to select substitution models and number of partitions based upon Bayesian information criterion (BIC) scores (Lanfear *et al.* 2012).

PartitionFinder partitioned COI by codon position with the following substitution models GTR+G, F81, GTR+G and partitioned ITSI as a single partition with K80+G substitution model. I used BEAST v2.4.6 (Bouckaert *et al.* 2014) for a Bayesian inference of phylogeny and RAxML v8.2.10 (Stamatakis 2014) for maximum likelihood phylogenetic analyses in the CIPRES Science Gateway (Miller *et al.* 2010).

In BEAST v2.4.6 loci were analyzed independently and in concatenation. Additionally, a concatenated analysis constraining a monophyletic *Lampsilis teres* (*L. teres* + *L. anodontoides*) was performed and a species tree analysis was conducted in *BEAST v2.4.6. A run consisted of a MCMC chain of 100,000,000 generations sampling every 5,000. A relaxed log-normal clock and a birth-death prior on speciation were used. A piecewise linear and constant root population size was used in my species tree analysis. Species assignments were based upon *a priori* morphological group identification (*L. teres* & *L. anodontoides*) and modern Unionidae taxonomy (Williams *et al.* 2017). Five or more independent runs were performed for each analysis. Runs were assessed for convergence and adequate mixing in Tracer v1.6.0 (Rambaut *et al.* 2014). I combined trees assuming a 30% burnin in LogCombiner v2.4.7 and generated a maximum clade creditability tree in TreeAnnotator v2.4.7 (Bouckaert *et al.* 2014).

My maximum likelihood analyses were conducted in RAxML v8.2.10 in CIPRES (Stamatakis 2014; Miller *et al.* 2010). Two outgroups species, *Amblema plicata* and *Fusconaia mitchelli*, were omitted from analysis. Three analyses were executed: one for each locus and one concatenated. Genes were partitioned identically to my Bayesian analyses but all partitions were assigned a GTR+G substitution model. Rapid bootstrapping of 100 iterations was conducted.

Population Genetics

Alignments of *L. teres* + *L. anodontoides* were analyzed to assess any relationship between genetic divergence and *a priori* morphological groups. The COI alignment was trimmed to a uniform length of 551 nucleotides. A TCS network (Clement *et al.* 2002) of COI haplotypes was constructed in the program PopART (Leigh & Bryant 2015). Separate COI alignments for *L. teres* and *L. anodontoides* were also assembled and separate analyses of molecular variances (AMOVA) were conducted to infer intraspecific differentiation between biogeographic regions. An ITSI alignment was trimmed to uniform length of 422 nucleotides. Gaps created by outgroup taxa were deleted from *L. teres* + *L. anodontoides* sequences. MEGA v7.0.25 was used to calculate uncorrected p-distances and diagnostic nucleotides (COI only) between groups (Kumar *et al*. 2016). An annotated mitochondrial genome of *Cristaria plicata* (GenBank accession: KM233451) was added to the alignment to decipher COI nucleotide positions *L. teres* and *L. anodontoides* sequences (Wang *et al*. 2016).

Morphometric Analysis

To quantitatively assess conchological differences between *a priori* morphological groups, I used *L. teres* and *L. anodontoides* specimens for which I had molecular and morphological material, a total of 87 specimens. Morphological characters were split into two datasets: traditional morphometric and geometric morphometric characters. Multivariate statistical analyses were performed and classification accuracies was assessed using two machine-learning algorithms.

Traditional Morphometrics

Maximum shell length (L), width (W), and height (H) posterior of the umbo were measured to the nearest 0.01mm using digital calipers. Specimens with lengths of <65mm were excluded because of potential allometric effects. Shell mass (M) of the right shell was measured using a digital scale to the nearest 0.001g. All measurements were log transformed. Shell color was categorically placed into 1 of 3 categories and presence/absence of green rays was scored by five individuals unfamiliar with the group to remove bias. Average scores were used then log transformed. The dataset was size corrected by taking ratios of log transformed measurements: H:W, L:H, centroid size (CS):M plus the two color characters for a total of five variables.

Geometric Morphometrics

In addition to traditional morphometric measurements I performed two dimensional geometric morphometrics (GM) analysis of shell shapes. Photographs were taken from a height of ~50cm using a camera stand and lightbox. The right valve was placed in black aquarium sand so that the interior outline of the shell was perpendicular to the camera lens. A three-axis bubble level was used to reduce parallax. I used the package "*geomorph*" (Adams *et al.* 2018) in the statistical software program R to digitize a total of 50 landmarks on the right shell (R Core Team 2013). An open outline was digitized with 45 semilandmarks placed approximately equidistant around the shell and landmarks at the beak & posterior end of the hinge to anchor the semi-landmarks, in addition to 3 internal landmarks. Prior to superimposition, each digitized specimen was visually inspected for accuracy using the *plotAllSpecimens* function in "*geomorph*". A

generalized Procrustes analysis (GPA) was conducted in "*geomorph*" to scale, translate, rotate, and align specimens (Adams *et al.* 2018). Semilandmarks were slid to minimize bending energy. Centroid size (CS) was calculated by taking the square root of the sum of squared distances between each landmark to the centroid. Additionally, separate analyses were conducted with the above dataset plus the *Lampsilis fallaciosa* holotype (USNM 30023a) (Figure 1.10) and 8 additional *L. anodontoides* specimens that lacked molecular data, in order to make inferences about the synonymy of *L. fallaciosa* and distribution of *L. anodontoides*. An additional dataset that contained the above dataset plus digitized illustrations was assembled to address taxonomic assignments. Separate GPAs were performed for each dataset.

Multivariate Analysis

Separate principal components analyses (PCA) using the covariance matrix of the traditional and GM datasets were performed in R and visualized in the package "*ggplot2*" (Wickham 2009). The traditional morphometric dataset was scaled prior to the PCA. To reduce the dimensionality of the GM dataset the first six principal component scores which described >95% of the variation in the dataset were extracted for downstream analyses. A two sample Hotelling's test with permutation (10,000) was conducted on each dataset using the package "*Hotelling*" to test for mean morphological group differences (Curran 2017).

Machine-Learning Classification

Prior to machine-learning classification analyses the GM and traditional datasets were combined. I used two machine-learning algorithms to assess morphological group classification accuracy. Specifically, the combined dataset was used as input into two machine learning classification models: Support Vector Machines (SVM) and Classification Trees (CT), as implemented in the packages "*e1071*" (Meyer & Wein 2017) and "*rpart*" (Therneau *et al.* 2018) in R (R Core Team 2013). Twenty iterations were conducted for both models. In each iteration the dataset was split in half and specimens were randomly put into a training or testing dataset. Each model was trained on the same training dataset and classification accuracies were computed when the model was run on the testing dataset. A bifurcating decision tree was produced at each iteration by the CT model. A similar analysis was conducted for my expanded morphology only dataset; however, since only GM was used I used the first six PC scores (>95% of variation) as input and split specimens with molecular data into the training dataset and morphology only specimens into the testing dataset. This procedure was also used for classifications of data from the taxonomic literature where digitized diagrams and shell measurements from the literature were used as data input.

RESULTS

Genetic Analyses

Molecular Phylogenetics

I sequenced the mitochondrial locus COI from 85 individuals of *L. teres* and 23 individuals of *L. anodontoides*. I sequenced the nuclear locus ITSI from a subset of individuals from each taxonomic group. All phylogenetic analyses failed to resolve a monophyletic '*Lampsilis teres'* (*L. teres* + *L. anodontoides*) as it is currently recognized (Figure 1.2-.7). However, *L. teres* and *L. anodontoides* were each well resolved as monophyletic with high support (>0.85 posterior probability) in all Bayesian analyses with exception of the ITSI gene tree analysis where *L. teres* was paraphyletic with respect to the closely related species *L. floridensis* (Figure 1.2). Maximum likelihood analyses recovered *L. anodontoides* as monophyletic with high support (99 or greater bootstrap values) in all analyses aside from the ITSI gene tree analysis where the tree formed a polytomy containing all *Lampsilis* species and *Villosa lienosa*. Similarly to the Bayesian ITSI gene tree, maximum likelihood analysis of the ITSI locus found *L. teres* paraphyletic with respect to *L. floridensis*: in all other analyses *L. teres* exhibited a sister group relationship with that species. My Bayesian concatenated analysis where '*L. teres*' (*L. teres* + *L. anodontoides*) was constrained to be monophyletic had a significantly worse marginal likelihood than the unconstrained Bayesian concatenated analysis (constrained = -4142.152, unconstrained = -4129.606). Although not close to *L. teres*, the precise position of the *L. anodontoides* clade is unclear. Both COI gene trees, maximum likelihood concatenated, and species tree analyses found *L. anodontoides* to be sister to a

L. siliquoidea, *L. hydiana*, *L. straminea* clade (Figures 1.2,1.4,1.6-7). While the Bayesian concatenated tree resolved *L. anodontoides* as sister to *Villosa lienosa* with low support and the Bayesian ITSI gene tree found *L. anodontoides* to be the sister group to all *Lampsilis* species included in the analysis.

Population Genetics

My TCS haplotype network for COI illustrates substantial genetic divergence between *L. anodontoides* and *L. teres* (Figure 1.8). Several river basins are represented by individuals of both species, and each species exhibits at least some genetic structure that correlates with geography. Results from the hierarchical nested AMOVA indicated significant intraspecific differentiation in both species between the Mississippian region (Upper & Lower Mississippi, Ohio, Tennessee-Cumberland, and Interior Highlands) and isolated gulf basins (Mobile Basin, Pearl-Pascagoula, Sabine-Trinity, and Western Gulf) (*L. teres* among region variation=72.485%, $P<0.001$, *L. anodontoides* $P<0.001$). Computed mean uncorrected p-distances between the *L. teres* and *L. anodontoides* groups were COI=7.9% (within *L. teres*=0.4%, *L. anodontoides*=0.6%) and ITSI=1.5% (within group [both]=0.1%). Thirty-three diagnostic nucleotide positions were identified in COI between groups with no amino acid changes detected.

Morphometric Analyses

Morphology datasets included 68 *L. teres* and 19 *L. anodontoides* specimens. The PCA results show much greater separation between species for the traditional morphometric dataset primarily across the first principal component axis (40% of

variation) (Figure 1.9). The variable height:length has the greatest loading on PC 1 (0.64) followed by mass:centroid size (0.44), color (-0.40), rays (-0.39) and width:height (-0.30). The GM PCA shows less separation between species however a clear pattern exists between PC 1 & 2 (77.5% of cumulative variation) (Figure 1.9). The Hotelling T^2 test with permutation showed a significant difference between groups for both the GM (T^2=160.56, P< 0.001) and traditional (T^2=279.18, P< 0.001) datasets.

The average classification accuracies of the machine learning algorithms were SVM=97.84% (kappa=93.34%) and CT=91.93% (kappa=78.23%). Classification trees most commonly produced decision trees splitting taxon groups by a single character, height:length. My expanded dataset including specimens for which I only had morphological data yielded results largely consistent with their *a priori* identifications: machine-learning algorithms indicated high classification accuracy for these specimens (SVM=9/9 and CT=6/9). However, my expanded dataset that included morphometric data from original species descriptions and other taxonomic literature grouped all three species descriptions (*L. teres* Rafinesque, *L. anodontoides* Lea, and *L. fallaciosa* Smith) together, indicating that *L. teres* has been described three separate times (Table 1.2). Taxonomic literature that used morphometric characters consistent with what I recognize to be *L. anodontoides* first appeared in Smith 1899. Since then, *L. anodontoides* has only been applied to specimens with shell morphology consistent with the lineage used herein.

DISCUSSION

In this study, I test for genetic structure among morphological variants of *L. teres* that have historically been classified as subspecies or distinct species. An exhaustive sampling of the known distribution of morphological variants, multilocus molecular phylogenetics, and two morphometric approaches revealed two divergent lineages (Figures 1.2-8) living in sympatry across multiple biogeographic zones (Figure 1.1). Although clear interspecific morphological differences exist (Figure 1.9) outliers in both species groups prevented 100% classification accuracy. Despite this, given the clear genetic distinctiveness of these lineages I again recognize *L. anodontoides*, providing a new description and neotype designation below.

Phylogeny and Species Boundaries

All but one phylogenetic analysis independently recovered a well-supported, monophyletic *L. anodontoides*. My molecular phylogenetic analyses show no evidence of hybridization or even a sister relationship between *L. anodontoides* and *L. teres*. *Lampsilis teres* was resolved as monophyletic in all phylogenetic analyses except ITSI gene trees where the species was paraphyletic with *L. floridensis*. However, as others have noted (Pfeiffer *et al.* 2016; Smith *et al.* 2018), incomplete lineage sorting is common in nuclear gene trees, specifically ITSI, between species with shallow divergences. Sequences of *L. anodontoides* were monophyletic for both markers. Importantly, genetic variation between *L. anodontoides* and *L. teres* is not due to isolation in allopatry (Figures 1.1,1.8), with a number of sympatric and even syntopic sites having

been identified. Clade membership of individual specimens corroborates *a priori* morphological designations (Figures 1.2-6,1.9).

My molecular dataset supports Williams *et al.*'s (2008) resurrection of *Lampsilis floridensis*. *Lampsilis floridensis* forms a well-supported monophyletic clade (>0.85 posterior probability or 80 or greater bootstrap value) in all phylogenetic analyses. Divergence between *L. teres* and *L. floridensis* likely arose through allopatric speciation from the separation of eastern gulf coast (drainages east of Mobile Basin) and Mobile Basin drainages. Additionally, my dataset shows evidence of divergence between these drainages in *L. straminea*. However, my sample size is insufficient to test species limits in that group. *Lampsilis hydiana* is also paraphyletic in my concatenated and COI trees, consistent with previous results. Misidentification is always a possibility when using GenBank sequences but my results support Harris *et al*.'s (2004) findings that *L. hydiana* is a species complex made of at least three taxa. Further phylogeographic analysis and integrative species delimitation methods are needed to determine the taxonomic status of *L. straminea* and *L. hydiana*.

Population Genetics

Results of the AMOVA and the TCS haplotype network demonstrate clear structure between *L. anodontoides* individuals from the Upper Mississippi/Ohio regions and the Sabine-Trinity leaving open the possibility that *L. anodontoides* contains additional cryptic taxa (Figures 1.1, 1.8). The Sabine-Trinity and Western Gulf regions exhibit high freshwater mussel endemism (12% & 35% of species endemic) so it would not be surprising if these *L. anodontoides* specimens represent an undescribed lineage

(Haag 2010). However, given the resolution of my sampling, it is impossible to tell if this variation is intra or inter-specific. Greater sampling is needed across the greater Mississippian region to characterize genetic variation in *L. anodontoides*.

This is the first phylogeographic study of *L. teres*. The TCS haplotype network of COI displays very little genetic variation in the Mississippi Basin (Upper & Lower Mississippi, Tennessee-Cumberland, Ohio, and Interior Highlands; Figure 1.8) indicating that this species disperses well. Although this is consistent with other phylogeographic studies of widespread Mississsippian species (Elderkin *et al.* 2006; Elderkin *et al.* 2008; Burdick & White 2007). By contrast, specimens collected from isolated gulf coast drainages (Western Gulf, Mobile Basin, and Pearl-Pascagoula) exhibit comparatively higher genetic structure (Figure 1.8). Surprisingly, specimens collected from the Western Gulf and Mobile Basin exhibit haplotype sharing as well as divergent haplotypes within populations. This is an interesting pattern given the geographic distance and isolation by saltwater between these regions. I speculate that haplotype sharing is due to dispersal of *L. teres* hosts, *Lepisosteus* sp., between drainages. It is well known the members of the Family Lepisosteidae can tolerate salinity and its possible inoculated individuals with encysted *L. teres* glochidia traveled between the Mobile Basin and Western Gulf basins. Comparative phylogeography of *L. teres* and its *Lepisosteus* hosts would be necessary to adequately test this hypothesis.

Morphometrics

The results of my morphometric analyses indicate *L. teres* and *L. anodontoides* exhibit distinct shell morphology that is diagnosable with high (though not perfect)

accuracy. However, although clear clustering of each species exists on both PCA plots (Figure 1.9), there is still some overlap of morphologies due to a few outlier specimens. Principal components analysis of traditional morphometric characters appeared to perform better than geometric morphometric approaches in separating species. Specifically, the characters height:length, shell mass:centroid size, color and the presence/absence of rays were informative for species identification. Sexual dimorphism, exhibited by both species, may be one reason geometric morphometrics was less successful at separating species shell morphology. However, the timely process of examining each specimen's gonads to sex individuals was not performed and thus sex is not a character used in these analyses. Furthermore, conchological sexual dimorphism patterns specifically in *L. teres* can be cryptic and sex determination based upon shell morphology alone can lead to misclassification (Hess *et al.* 2018).

Finally, interspecific shell morphology differences in the Sabine-Trinity and Western Gulf regions were more cryptic. I noticed that *L. anodontoides* specimens collected in the Sabine-Trinity region had slightly lower height:length and mass:centroid size ratios. Conversely, multiple *L. teres* specimens collected from both the Sabine-Trinity and Western Gulf had height:length ratios that overlapped considerably with the *L. anodontoides* specimens collected from these regions. However, my sample sizes from this region are very small (*L. anodontoides* n=2, *L. teres* n=5) and more collecting needs to be done to characterize morphological variation in the region.

Distribution & Conservation

The distributional ranges of these species groups overlap extensively and in one location (Neches River) they were collected syntopically (Figure 1.1). The full distribution of *L. anodontoides* remains largely unknown. Lea (1831) listed the Mississippi, Ohio, and Alabama rivers as type localities for *L. anodontoides*. However, these type locality designations are invalid, as my morphological classification analyses unanimously indicate that the original description of *L. anodontoides* was in fact a redescription of *L. teres* (Table 1.2). My dataset for this species includes individuals from the Upper Mississippi (Embarrass, Illinois, Iowa, Mississippi, and Wisconsin rivers) Ohio (Ohio River), and the Sabine-Trinity (Neches River) regions. My morphology only dataset and subsequent classification indicates that *L. anodontoides* historically occurred in other biogeographic regions including the Tennessee-Cumberland, Lower Mississippi and Great Plains. Williams *et al.* 2008 noted that *L. anodontoides* specimens are known from the Mobile Basin: workers in these regions should be aware of the possible presence of this species.

Lampsilis anodontoides was rare wherever I could collect them with exception to certain reaches in the Embarrass River, eastern Illinois. Personal communication with other malacologists across North America and visits to museum collections confirmed this observation. In Iowa, Ohio, and Wisconsin where I have demonstrated *L. anodontoides* occurs*, L. teres* is listed as threatened or endangered. Smith (1899) indicated that *L. anodontoides* was extremely important to the button industry in the Upper Mississippi region and that it once was the most abundant species of the "sand shells". Mathiak (1979), reporting on a survey of the Wisconsin River, remarked that *L.*

anodontoides “is a rare clam now”. This species is rare and a serious conservation assessment is needed.

Conclusions

Cryptic diversity in freshwater bivalves remains problematic. As I have demonstrated here, sympatric, divergent cryptic species that likely have different life histories, host use, and habitat requirements are being managed as a single taxon. This study is one of a growing volume of unionid research that demonstrates small variation in shell morphology can correlate to deep phylogenetic divergence (Kuehnl 2009; Smith *et al.* 2018). For a group as imperiled as freshwater mussels, this is an obvious conservation management concern, particularly with the growing popularity of propagation and translocation as conservation management tools. Over a dozen propagation facilities are in operation in the United States with little to no genetic assessment of managed stocks (FMCS 2016). Ideally translocation and propagation action plans would include a genetic component verifying the validity of the source stock choice. Even in the best-studied freshwater mussel fauna in the world, this study illustrates that North American malacology is still in the early stages of determining species richness and species boundaries even in wide ranging species.

SPECIES ACCOUNTS

Untangling the taxonomy of these two lineages in the absence of type specimens and abstract species descriptions proved frustrating. These factors were compounded when the acceptance of authors' species designations have fluctuated over time. The source of this confusion stems from Rafinesque's species descriptions and a wavering of acceptance and rejection of his names. Based upon the species descriptions of Rafinesque (1820), Lea (1831), and Smith (1899), I am confident that all three authors were describing the same species (Table 1.2), *L. teres*. However, to prevent further confusion I have chosen to retain *L. anodontoides* Lea (1831) as the name has been tied recently to morphological characters consistent with *L. anodontoides* as described herein. I designate neotypes for both lineages (*L. teres* & *L. anodontoides*) and a brief 'redescription' using these neotype designations. A special thanks to the developers and maintainers the MUSSELp Database (Graf & Cummings 2018) as it provided an excellent resource to decipher the taxonomic history of these two species.

***Lampsilis anodontoides* Lea (1831)**

Type Material: Neotype: JFBM 22433, length 127.26mm, height 64.28mm, width 45.66mm (Figure 1.14). The holotype has apparently been lost from Lea's collection: holdings at USNM of Lea material were thoroughly searched but the holotype could not be found. I designate a neotype for the species collected from the Embarras River at Fox Ridge State Park, 7 miles south of Charleston, IL (39.408800, -88.170600).

Diagnosis: I tentatively place this taxon in the genus *Lampsilis* based upon phylogenetic relationships to other members of the genus. However, Bayesian concatenated phylogenetic analysis suggests a sister relationship with *Villosa lienosa* with low posterior probability (0.095). Additionally, unionid systematic studies have recovered paraphyly at the generic level of both *Lampsilis* and *Villosa* (Campbell *et al*. 2005; Graf & O'Foighil 2000; Kuehnl 2009). Further phylogenetic studies with greater taxon sampling are necessary for changes to generic taxonomy.

At the COI locus, *L. anodontoides* can be distinguished from *L. teres* by 33 nucleotide substitutions and distinguished from *Villosa lienosa* and all other *Lampsilis* species used in this study by 12 nucleotide substitutions (219:C, 237:A, 249:A, 312:T, 393:A, 423:C, 474:C, 501:C, 510:G, 531:A, 570:C, 579:C). Conchologically, *L. anodontoides* could only be confused with *L. teres*. However, *L. anodontoides* tend to be more circular in shell outline: H:L 85.7% (82.8%-87.4%) than *L. teres* 82.6% (79.9%-85.1%) and a thicker shell: M:CS 74.8% (63.3%-80.6%) versus 58.3% (33.5%-75.6%). Lastly, participants consistently scored *L. anodontoides* shells as more 'yellow': 1.43 out of 3 (1-2.6) versus 2.28 (1-3). Unfortunately, there is considerable overlap in each of

these morphological characters. However, when used in combination, shell shape, thickness, and color, are highly informative and highly (if not perfectly) diagnostic.

Description: *Shell* – ovate to circular in valve outline; thick, very robust; moderately inflated; posterior margin pointed dorsally, rounded or bluntly pointed; ventral margin rarely straight; umbo positioned 30-40% of the total length; umbo indistinctly sculptured or with discontinuous ridges (only observed in juveniles) (Figure 1.13); umbo cavity wide, shallow; pseudocardinal teeth robust, single tooth in right valve often wider than erect with broad, flat top; two pseudocardinal teeth in left valve, posterior tooth erect and nearly vertical, anterior tooth horizontal and compressed; lateral teeth straight or nearly so; one lateral tooth in right valve that is erect, blade-like, almost sharp; two lateral teeth in left valve with deep crevice; inside nacre white or salmon; outside periostracum vibrant yellow or a stained khaki; green rays only present in young individuals.

Soft body – mantle gray to white; mantle flap present, on anterior end of flap is a serrated extension that may mimic a 'tail' (n=7), no visible 'eyespot', pigmentation nondescript; foot white, very robust; labial palps white to gray; inner gills white, ~70% of mantle length, gill height 30-40% of gill length; outer gills marsupial; in gravid female (n=2) posterior portion of outer gill extremely swollen in single lobe with prominent black stripe; incurrent aperture at least twice the length of excurrent aperture.

Distribution: Extant populations confirmed in the Ohio, Upper Mississippi, and Sabine-Trinity biogeographic regions. However, museum visits suggest its historic presence in other faunal zones including the Lower Mississippi: Black River (UMMZ-MC 83116 & 83755) and St. Francis River (UMMZ-MC 130097), Great Plains: Lyons

Creek (UMMZ-MC 83104) and Mussel Fork (INHS 82899), and Tennessee: Tennessee River (INHS 14527).

Conservation Status: Unknown. Appears to be locally common in the Embarrass River: it may be common in other Upper Mississippi and Ohio rivers. Collecting efforts and personal communication with other malacologists suggests it is a rare species that deserves conservation attention.

***Lampsilis teres* Rafinesque (1820)**

Synonyms: *Lampsilis fallaciosus* = *L. fallaciosa* Smith, 1899, Bull. U.S. Fish. Comm.: 291, pl. 79.

Type Material: Neotype: JFBM 22421.1, length 110.23mm, height 43.03mm, width 44.25 (Figure 1.12). Holotype has been lost. I designate a neotype for the species collected from the Mississippi River at Beaver Island near Camanche, Iowa (41.796955, -90.219580). Rafinesque's (1820) type specimen was collected in the Wabash River presumably in Indiana or eastern Illinois. The type of *Lampsilis fallaciosa* (Smith 1899) (USNM 30023a; Figure 1.10) was collected from the Ohio River in Sedamsville, Ohio. The United States National Museum lists this specimen as the holotype of *L. teres* but they are undoubtedly referring to *L. fallaciosa*.

Diagnosis: *Lampsilis teres* resembles *L. anodontoides* and sister species *L. floridensis*. See above *L. anodontoides* diagnosis to distinguish between *L. teres* and *L. anodontoides*. *Lampsilis teres* differs from *L. floridensis* at the COI locus by twelve nucleotide substitutions (148:T, 153:T, 207:A, 282:A, 333:T, 381:T/C, 429:T, 519:A,

538:T, 558:C/A, 630:G, 633:T). *Lampsilis teres* shells appear to be moderately thicker and sexual dimorphism is more apparent in *L. teres*. *Lampsilis teres* (Mississippian) and *L. floridensis* (Eastern Gulf) have allopatric distributions.

Description: *Shell* – cylindrical in valve outline and antero-posteriorly; shell moderately thick to thin (only found in TX specimens); moderately inflated; posterior margin bluntly pointed medially or dorsally; ventral margin straight and long; umbo positioned anteriorly 15-25% of the total length; umbo sculptured with fine wavy ridges (more common in specimens from Upper Mississippi biogeographic region) (Figure 1.11); umbo cavity wide, modestly deep; pseudocardinal teeth moderately erect, single triangular tooth in right valve, two teeth in left valve that are nearly in parallel, diagonal; lateral teeth nearly straight; one erect lateral tooth in right valve, blade-like; two lateral teeth in left valve, ventral tooth slightly more erect; inside nacre varies from white, salmon, light pink; periostracum varies from chestnut, bronze, straw, bleached yellow, sometimes with green rays.

Soft body – mantle tan to white; mantle flap present in females, no visible 'eyespot' or 'tail', pigmentation nondescript, some individuals from Duck (n=4), Cache (n=2), Hatchie (n=1), Mississippi (n=2), Saline (n=1) rivers and Okatibbee Reservoir (n=1) have a bright reddish-maroon stripe on inside mantle flap; foot white to khaki; labial palps white to gray; inner gills pinkish-gray, ~70% of mantle length, gill height 20-40% of gill length; outer gills marsupial; in gravid females (n=4) posterior portion of outer gill extremely swollen with prominent black stripe divided into two lobes, a larger medial lobe and a reduced posterior lobe; excurrent aperture ranges in length between 50-100% of incurrent aperture.

Distribution: Widespread throughout the Mississippian region aside from the St. Lawrence-Great Lakes faunal zone. Absent from the Atlantic Slope and Eastern Gulf.

Conservation Status: Considered stable (Williams *et al*. 1993) however it is listed as endangered in Wisconsin, Minnesota, Iowa, Ohio and critically imperiled in West Virginia.

Table 1.1. Collection localities with sample sizes for molecular and morphological data.

Species	Voucher	River (Geographic Province)	Latitude	Longitude	COI	ITSI	Morphology
Lampsilis teres	JFBM 22422	Bogue Chitto Creek (Mobile Basin)	32.30629	-87.28015	7	4	7
Lampsilis teres	JFBM 22425	Black Warrior River (Mobile Basin)	32.631697	-87.811349	10	3	10
Lampsilis teres	JFBM 22427	Okatibbee Reservoir (Pascagoula)	32.521786	-88.808334	1	1	1
Lampsilis teres	JFBM 22428	Saline River (Lower Mississippi)	33.346099	-91.983193	10	1	10
Lampsilis teres	ASUMZ 1208	Strawberry River (Interior Highlands)	36.02795	-91.32545	7	0	7
Lampsilis teres	JFBM 22429	Duck River (Tennessee)	35.618385	-87.024758	5	0	5
Lampsilis teres	JFBM 22431	Cache River (Ohio)	37.466389	-89.076667	6	3	6
Lampsilis teres	INHS 35066	Cache River (Ohio)	37.466389	-89.076667	5*	0	5
Lampsilis teres	INHS 25571	Ohio River (Ohio)	38.34065	-85.64205	1*	0	0
Lampsilis teres	INHS 24192	Mississippi River (Upper Mississippi)	42.61009	-90.69463	1*	0	0
Lampsilis teres	JFBM 22421	Mississippi River (Upper Mississippi)	41.796955	-90.21958	2	2	2
Lampsilis teres	JFBM 22435	Mississippi River (Upper Mississippi)	43.18511554	-91.14455717	4	4	4
Lampsilis teres	JFBM 22430	Hatchie River (Lower Mississippi)	35.241403	-88.922461	8	1	8
Lampsilis teres	JFBM 22434	Timber Creek (Upper Mississippi)	40.36061	-89.13652	1	0	1
Lampsilis teres	TAMU-NRI 8136	Rio Grande (Western Gulf)	27.732917	-99.776275	2	1	2
Lampsilis teres	TAMU-NRI 8137	Rio Grande (Western Gulf)	27.722883	-99.76258	2	1	0
Lampsilis teres	TAMU-NRI 8281	Rio Grande (Western Gulf)	27.60224	-99.58051	1	0	0
Lampsilis teres	TAMU-NRI 8165	Guadalupe River (Western Gulf)	28.830712	-97.055658	3	2	0
Lampsilis teres	TAMU-NRI 8174	Brazos River (Western Gulf)	29.645447	-95.95335	1	1	0
Lampsilis teres	TAMU-NRI 8223	Brazos River (Western Gulf)	30.378934	-96.161204	1	0	0
Lampsilis teres	TAMU-NRI 8329	Colorado River (Western Gulf)	29.67159	-96.458137	1	0	0
Lampsilis teres	TAMU-NRI 8281	Trinity River (Sabine/Trinity)	31.62574	-95.78813	1	0	0
Lampsilis teres	TAMU-NRI 8030	San Jacinto River (Sabine/Trinity)	30.42734	-95.12647	2	1	0
Lampsilis teres	TAMU-NRI 8052.1,4-5	Neches River (Sabine/Trinity)	30.643163	-94.051707	3	2	3
Lampsilis anodontoides	TAMU-NRI 8052.2-3	Neches River (Sabine/Trinity)	30.643163	-94.051707	2	2	2

Lampsilis anodontoides	JFBM 14984	Mississippi River (Upper Mississippi)	39.723876	-91.360834	2*	0	2
Lampsilis anodontoides	INHS 25524	Mississippi River (Upper Mississippi)	39.54019	-91.1461	1*	0	1
Lampsilis anodontoides	JFBM 22438	Embarrass River (Upper Mississippi)	39.409556	-88.171051	7	2	7
Lampsilis anodontoides	JFBM 22433	Embarrass River (Upper Mississippi)	39.4088	-88.1706	1	1	1
Lampsilis anodontoides	INHS 27760	Illinois River (Upper Mississippi)	39.7049	-90.6449	1	0	1
Lampsilis anodontoides	INHS 32440	Illinois River (Upper Mississippi)	39.797858	-90.592985	1*	0	1
Lampsilis anodontoides	INHS 32502	Illinois River (Upper Mississippi)	39.729788	-90.629918	1	0	1
Lampsilis anodontoides	INHS 32542	Illinois River (Upper Mississippi)	39.81948	-90.577144	1*	0	1
Lampsilis anodontoides	INHS 32555	Illinois River (Upper Mississippi)	39.632209	-90.606099	1*	0	1
Lampsilis anodontoides	JFBM 22439 & photo	Iowa River (Upper Mississippi)	41.672157	-91.562415	2	0	1
Lampsilis anodontoides	photo	Wisconsin River (Upper Mississippi)	43.200412	-90.428356	1	1	0
Lampsilis anodontoides	JFBM 4917	Wisconsin River (Upper Mississippi)	43.207247	-90.361692	1*	0	1
Lampsilis anodontoides	INHS 33464	Wabash River (Ohio)	38.9888	-87.5788	1*	0	1
Lampsilis fallaciosa	USNM 30023a	Ohio River (Ohio)	39.093333	-84.57305556	0	0	1
Lampsilis anodontoides	UMMZ 83104	Lyons Creek (Great Plains)	38.797774	-96.940463	0	0	1
Lampsilis anodontoides	UMMZ 83755	Black River (Lower Mississippi)	36.1024	-91.0975	0	0	1
Lampsilis anodontoides	UMMZ 130097	St. Francis River (Lower Mississippi)	35.532859	-90.424056	0	0	1
Lampsilis anodontoides	UMMZ 44896	White River (Ohio)	38.818727	-86.148295	0	0	1
Lampsilis anodontoides	UMMZ 83116	Black River (Lower Mississippi)	36.3	-90.8	0	0	1
Lampsilis anodontoides	INHS 9588	White River (Ohio)	38.524594	-87.324557	0	0	1
Lampsilis anodontoides	INHS 14527	Tennessee River (Tennessee)	35.222516	-88.261087	0	0	1
Lampsilis anodontoides	INHS 82899	Mussel Fork (Great Plains)	39.48616	-92.95228	0	0	1
Lampsilis teres	FLMNH 441218	GenBank			1	1	0
Lampsilis teres		GenBank			1	0	0
Lampsilis floridensis	JFBM 22437	Flint River (Apalachicola)	31.30919	-84.33491	10	2	0
Lampsilis hydiana	JFBM 22432	Cache River (Ohio)	37.466389	-89.076667	7	3	0
Lampsilis hydiana		GenBank			1	0	0

Lampsilis siliquoidea	JFBM 22440	Pomme de Terre (Upper Mississippi)	45.17964	-96.07845	2	1	0
Lampsilis siliquoidea		GenBank			1	0	0
Lampsilis siliquoidea		GenBank			1	0	0
Lampsilis straminea	JFBM 22423	Bogue Chitto Creek (Mobile Basin)	32.30629	-87.28015	1	1	0
Lampsilis straminea	JFBM 22424	Gantt Reservoir (Escambia)	31.42638	-86.45871	1	0	0
Lampsilis straminea	JFBM 22426	Sipsey River (Mobile Basin)	33.0782	-87.97529	1	0	0
Lampsilis straminea		GenBank			1	0	0
Amblema plicata	FLMNH 441152	GenBank			1	1	0
Fusconaia mitchelli	FLMNH 438010	GenBank			1	1	0
Leptodea fragilis	FLMNH 441212	GenBank			1	1	0
Leptodea fragilis		GenBank			1	0	0
Leptodea fragilis		GenBank			1	0	0
Villosa lienosa	FLMNH 441251	GenBank			1	1	0

*partial sequence

Table 1.2. Machine-learning classifications of historical literature descriptions of type and non-type material using geometric morphometrics of diagrams and traditional morphometrics of shell dimension ratios. CT = Classification Trees, SVM = Support Vector Machines.

Publication	Species Nomen	Evidence	CT	SVM
Rafinesque 1820*	teres	Traditional	*L. teres*	*L. teres*
Lea 1831*	anodontoides	Traditional	*L. teres*	*L. teres*
Lea 1831*	anodontoides	Geometric	*L. teres*	*L. teres*
Conrad 1836	teres	Geometric	*L. teres*	*L. teres*
Hanley 1842	anodontoides	Traditional	*L. teres*	*L. teres*
Baker 1898	anodontoides (m)	Traditional	*L. teres*	*L. teres*
Baker 1898	anodontoides (f)	Traditional	*L. teres*	*L. teres*
Smith 1899*	fallaciosa TYPE	Geometric	*L. teres*	*L. teres*
Smith 1899*	fallaciosa TYPE	Traditional	*L. teres*	*L. teres*
Smith 1899	anodontoides	Geometric	*L. anodontoides*	*L. anodontoides*
Call 1900	teres	Geometric	*L. teres*	*L. teres*
Simpson 1914	anodontoides (m)	Traditional	*L. anodontoides*	*L. anodontoides*
Simpson 1914	anodontoides (f)	Traditional	*L. anodontoides*	*L. anodontoides*
Simpson 1914	fallaciosa (m)	Traditional	*L. teres*	*L. teres*
Simpson 1914	fallaciosa (f)	Traditional	*L. teres*	*L. teres*
Utterback 1916	anodontoides (m)	Traditional	*L. anodontoides*	*L. anodontoides*
Utterback 1916	anodontoides (f)	Traditional	*L. anodontoides*	*L. anodontoides*
Utterback 1916	fallaciosa (m)	Traditional	*L. teres*	*L. teres*
Utterback 1916	fallaciosa (f)	Traditional	*L. teres*	*L. teres*
Baker 1928	anodontoides (f)	Traditional	*L. anodontoides*	*L. anodontoides*
Baker 1928	anodontoides (f)	Traditional	*L. anodontoides*	*L. anodontoides*
Baker 1928	anodontoides (m)	Traditional	*L. anodontoides*	*L. anodontoides*

Baker 1928	fallaciosa (m)	Traditional	*L. teres*	*L. teres*
Baker 1928	fallaciosa (f)	Traditional	*L. teres*	*L. teres*
Baker 1928	fallaciosa (m)	Traditional	*L. teres*	*L. teres*
Baker 1928	fallaciosa (f)	Traditional	*L. teres*	*L. teres*
Baker 1928	fallaciosa (m)	Traditional	*L. teres*	*L. teres*
Murray & Leonard 1962	anodontoides anodontoides	Geometric	*L. teres*	*L. anodontoides*
Oesch 1984	teres teres	Geometric	*L. teres*	*L. teres*
Oesch 1984	teres anodontoides	Geometric	*L. teres*	*L. anodontoides*

*Original species description

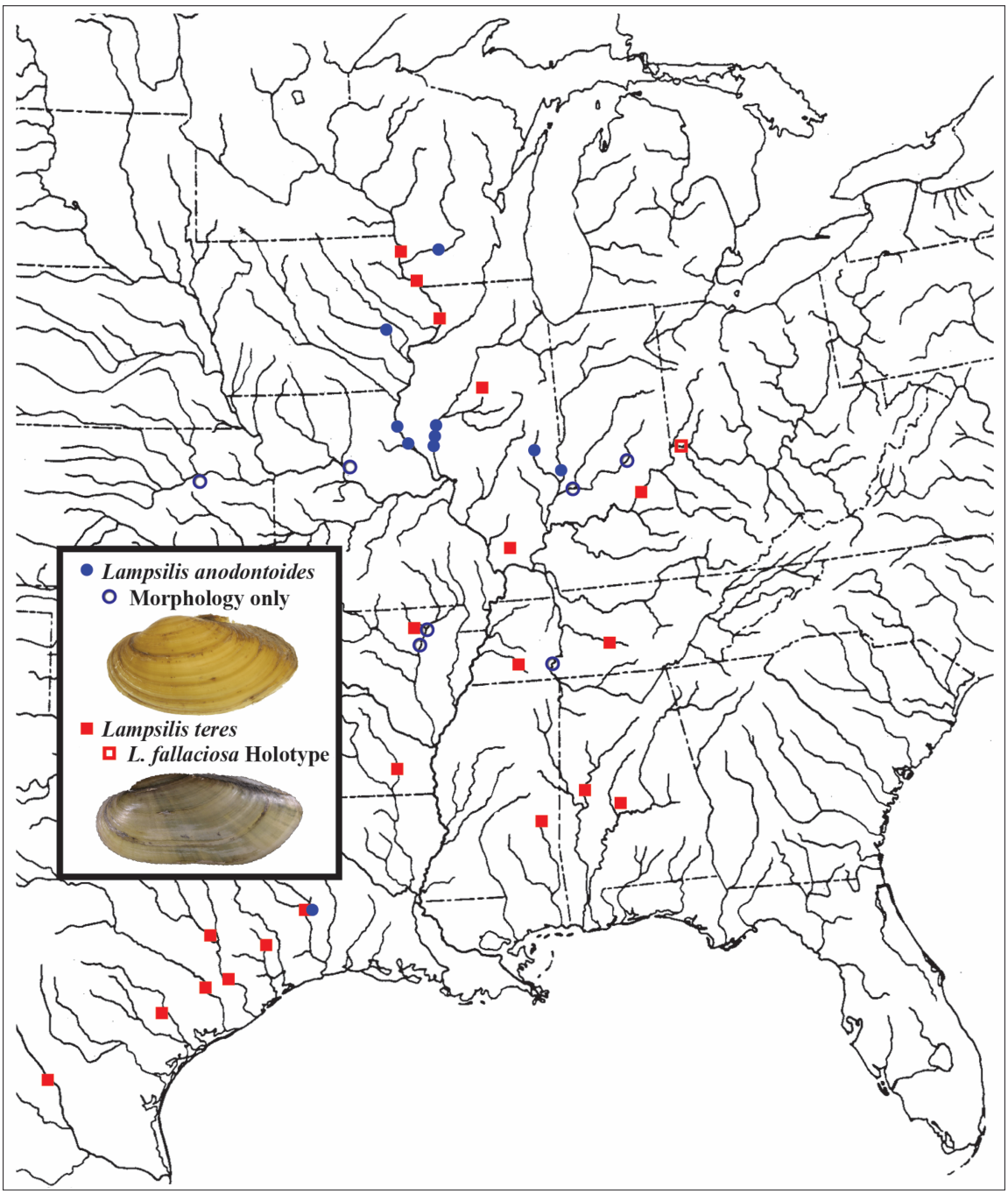

Figure 1.1. Map of sampling localities of *L. teres* and *L. anodontoides*. Pictured: *L. anodontoides* JFBM 22438 and *L. fallaciosa* holotype USNM 30023a.

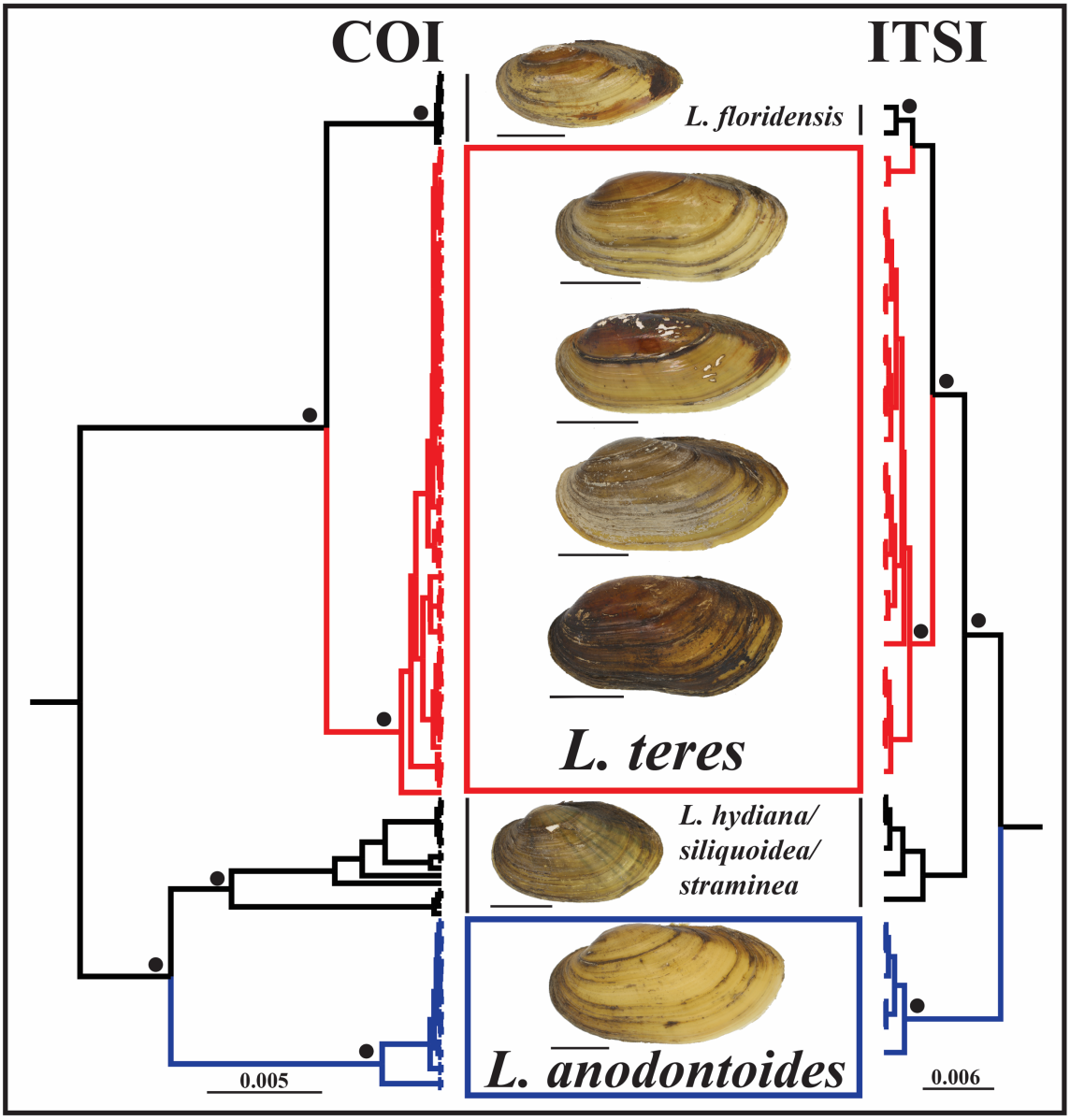

Figure 1.2. COI and ITSI Bayesian gene trees highlighting the genealogical relationships of *L. teres* and *L. anodontoides* and sister taxa. Outgroups more distantly related have been pruned from both gene trees. Black circles denote a posterior probability >0.85. Scale bar = 30mm. Pictured from top to bottom: *L. floridensis* JFBM 22437, *L. teres* JFBM 22435, JFBM 22431, TAMU-NRI 8136, ASUMZ 1208, *L. siliquoidea* JFBM 22440, and *L. anodontoides* JFBM 22433.

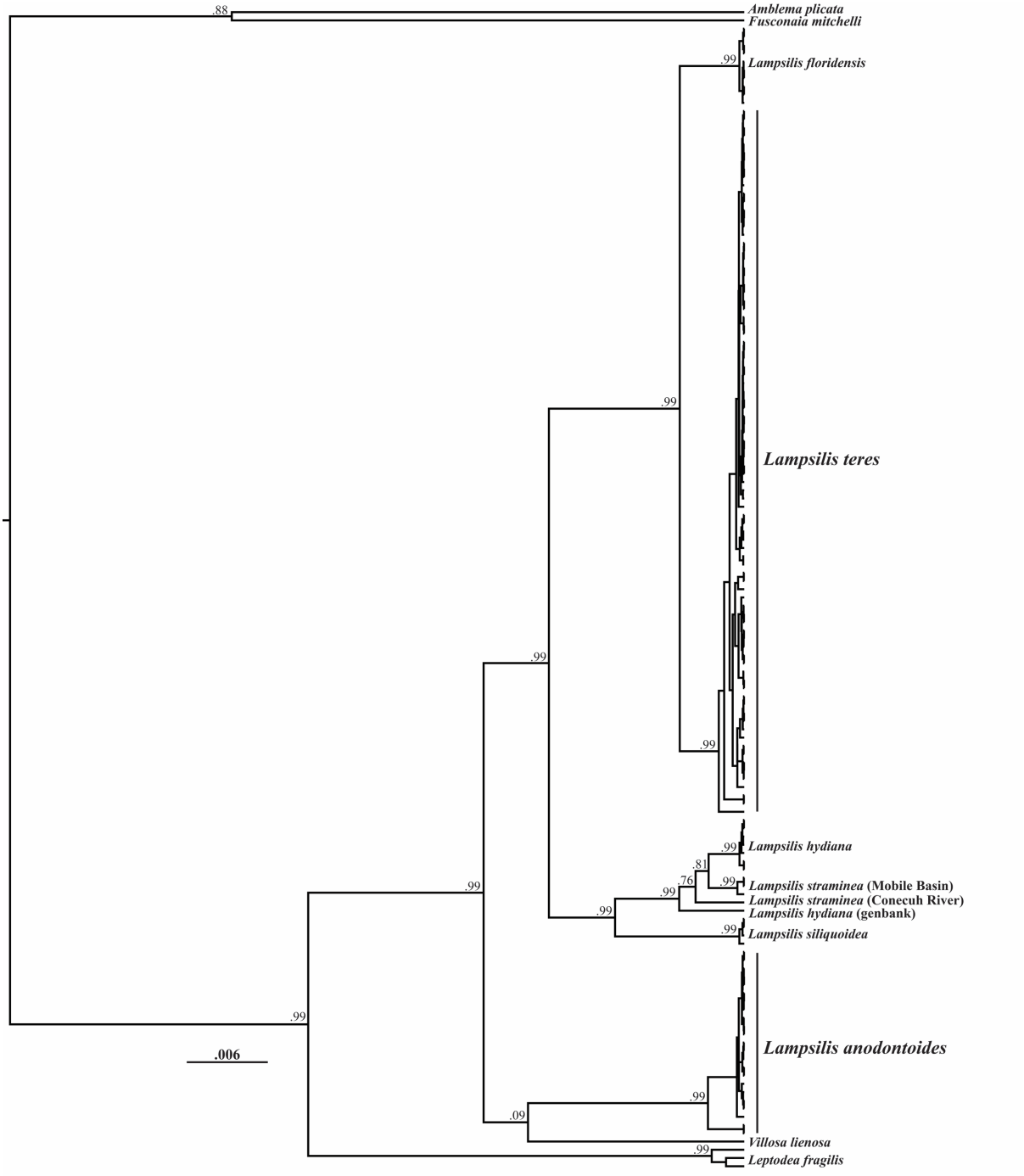

Figure 1.3. Phylogenetic hypothesis generated by Bayesian analysis using COI & ITSI loci in concatenation. Numbers above nodes indicate posterior probability.

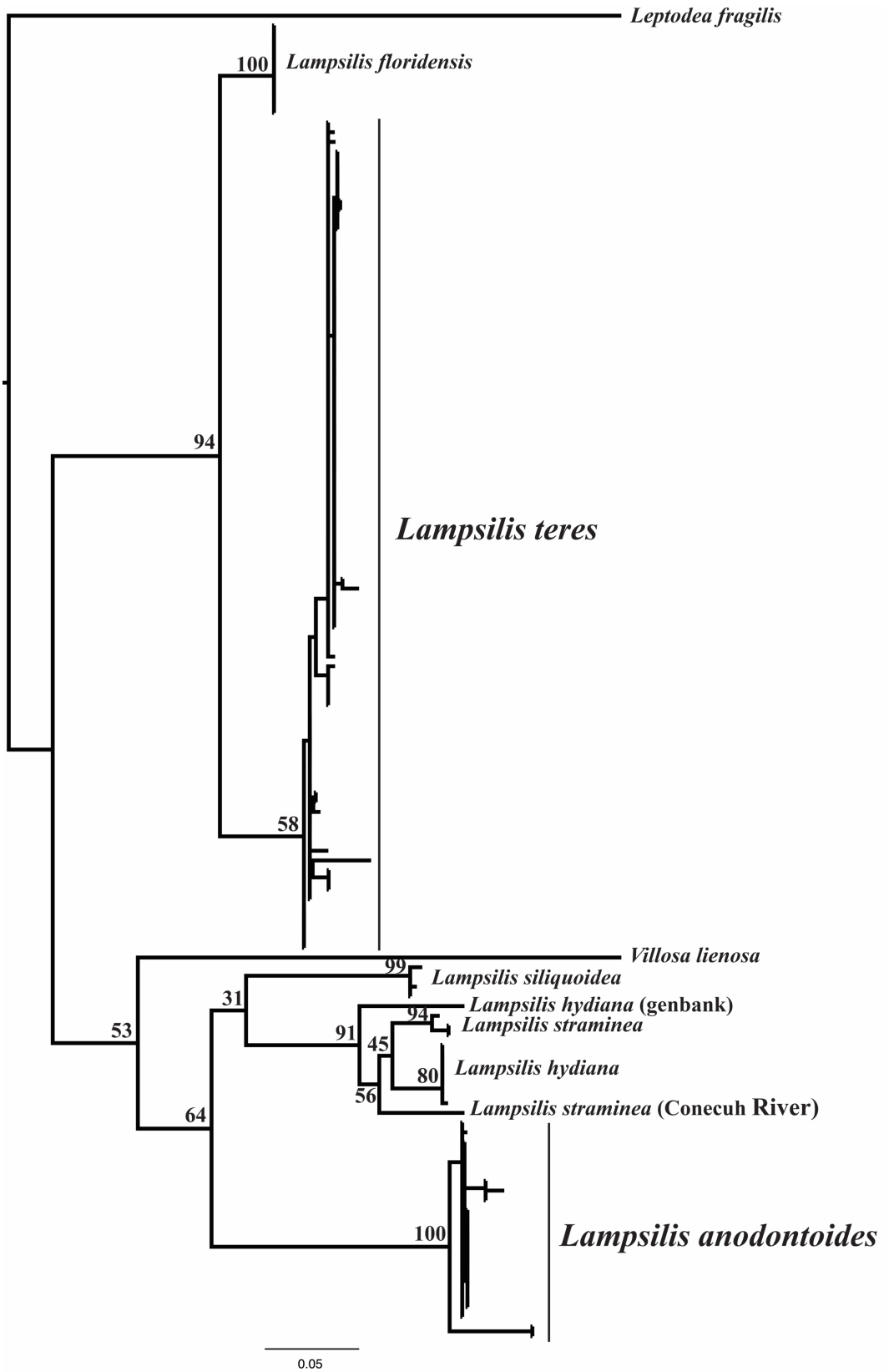

Figure 1.4. Maximum likelihood estimation of mtDNA COI gene tree. Numbers above nodes indicate bootstrap values out of 100.

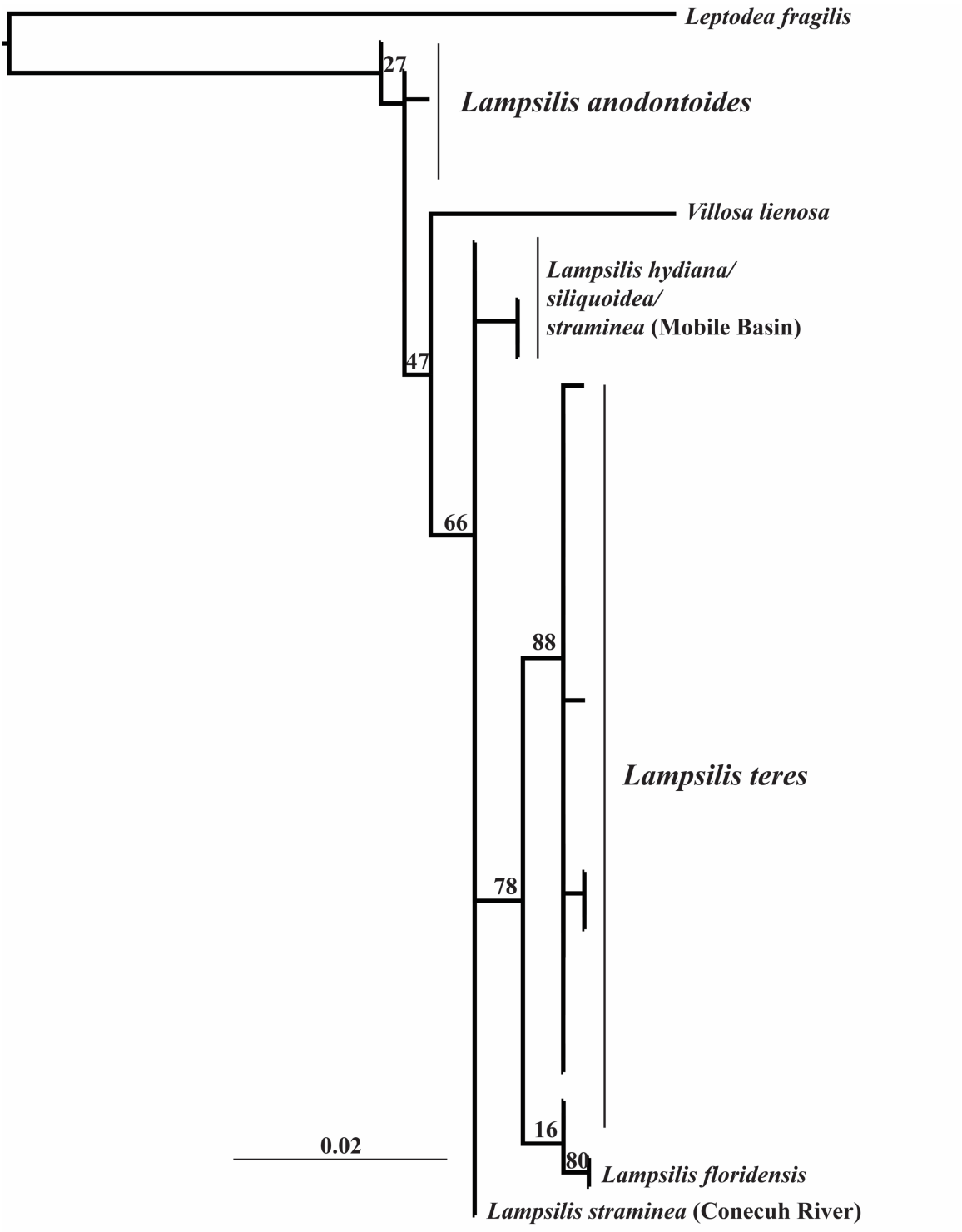

Figure 1.5. Maximum likelihood estimation of nuDNA ITSI gene tree. Numbers above nodes indicate bootstrap values out of 100.

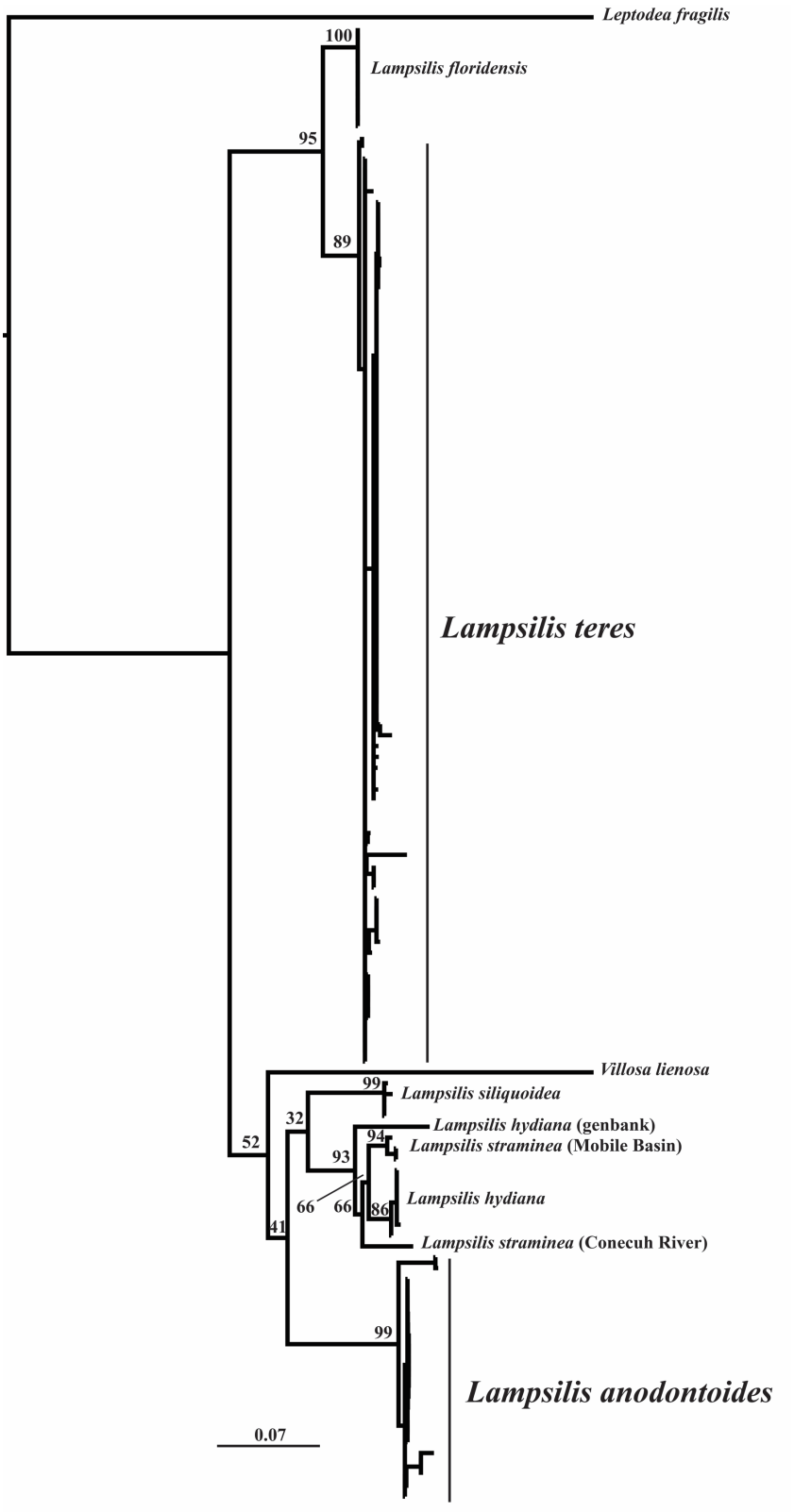

Figure 1.6. Maximum likelihood estimation of phylogeny using both COI & ITSI loci in concatenation. Numbers above nodes indicate bootstrap values out of 100.

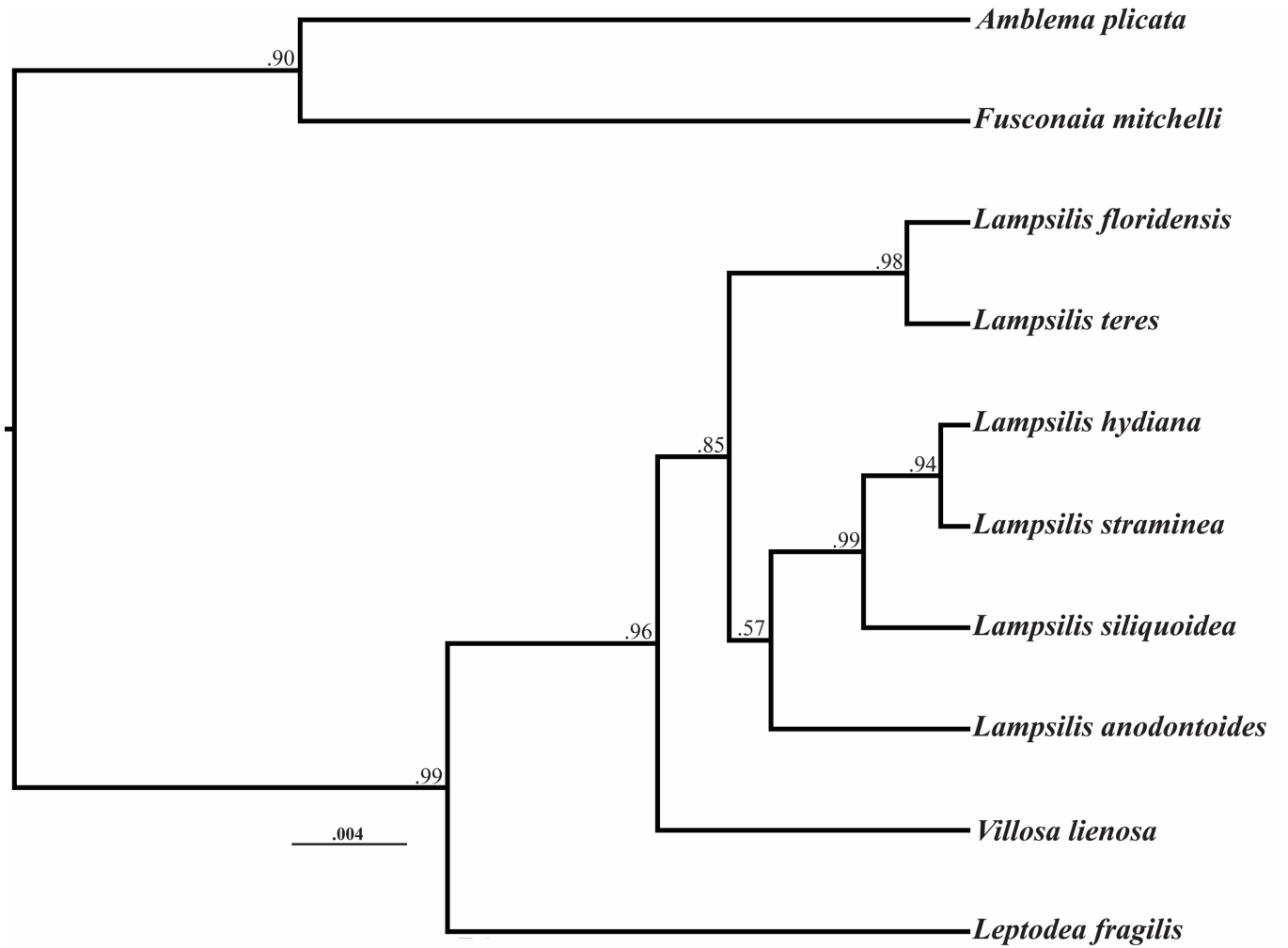

Figure 1.7. Phylogenetic hypothesis generated through a coalescent-based Bayesian species tree analysis. Numbers above nodes indicate posterior probability.

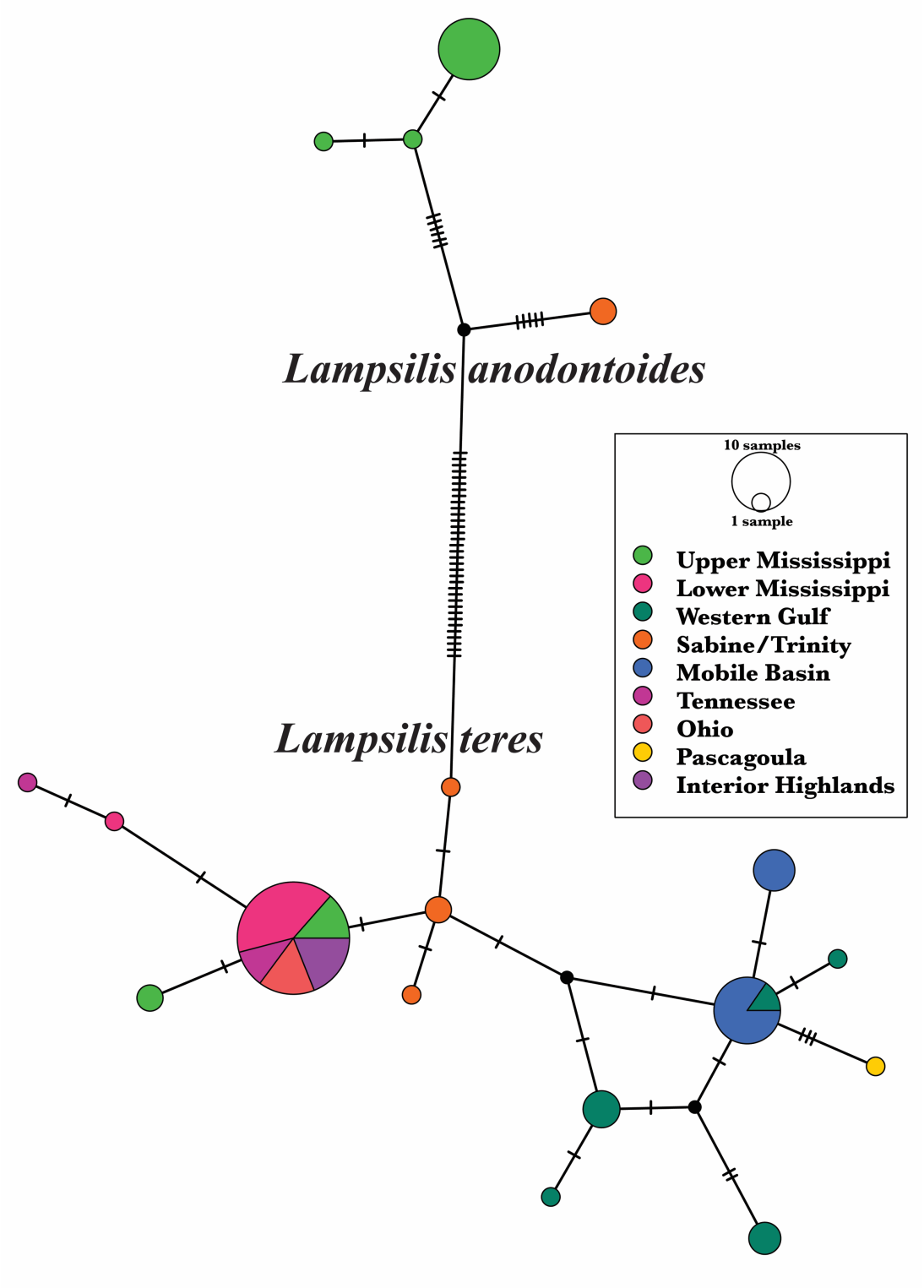

Figure 1.8. TCS haplotype network of the COI locus for *L. anodontoides* and *L. teres* showing intraspecific and interspecific genetic variation as it correlates to biogeographic regions defined by Haag 2010

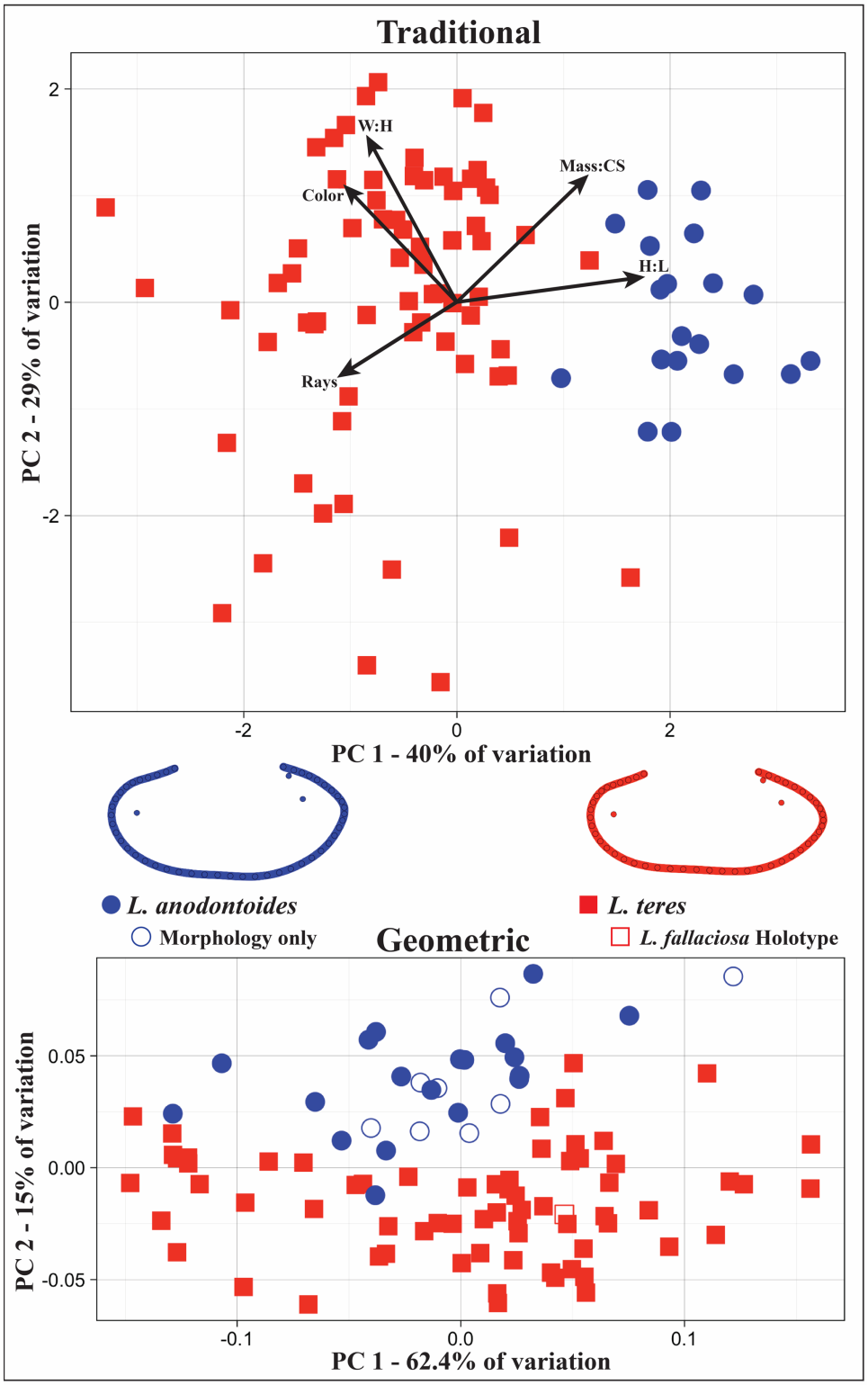

Figure 1.9. Principal component graphs from two PCAs of traditional and geometric morphometric characters. Between plots contains the mean digitized shape for each species.

Figure 1.10. *Lampsilis fallaciosa* (Smith 1899) type specimen (USNM 30023a).

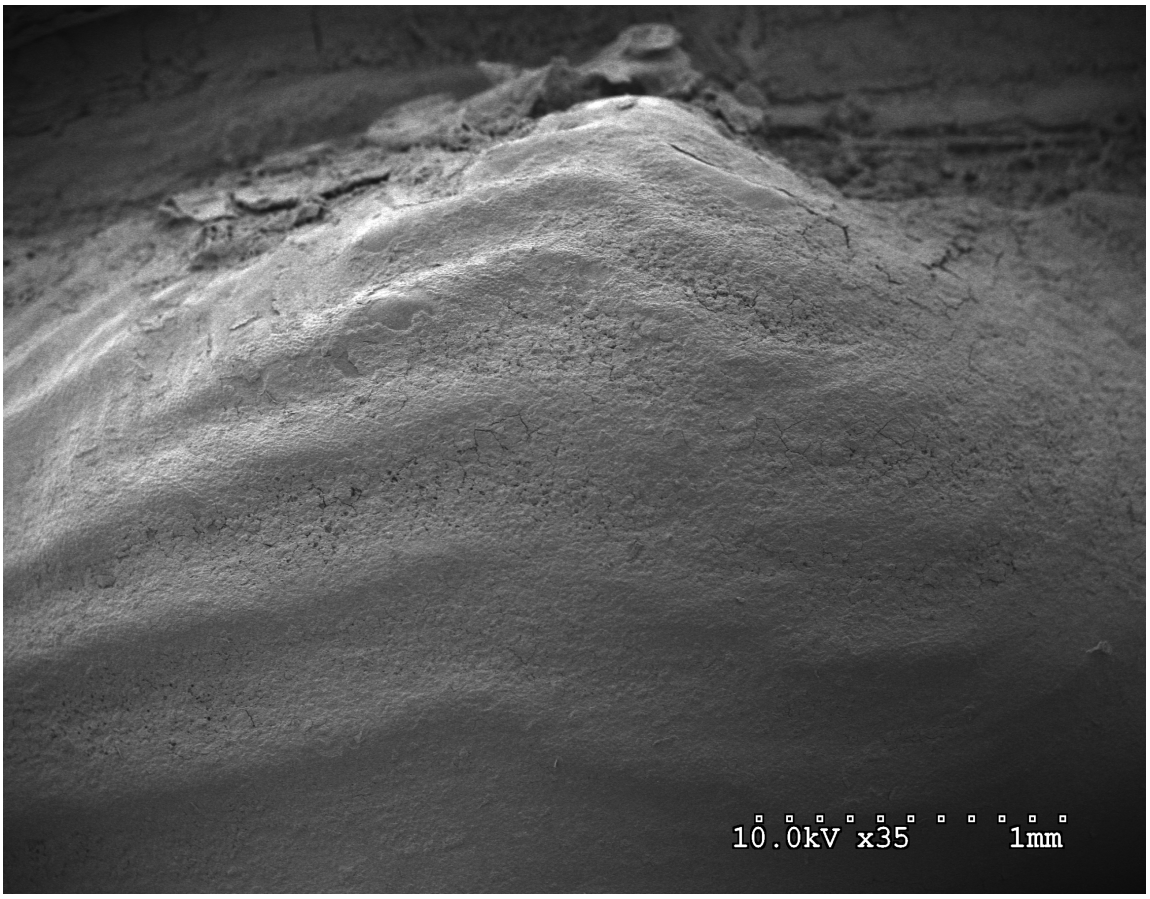

Figure 1.11. Beak sculpture of *L. teres* JFBM 22421.2.

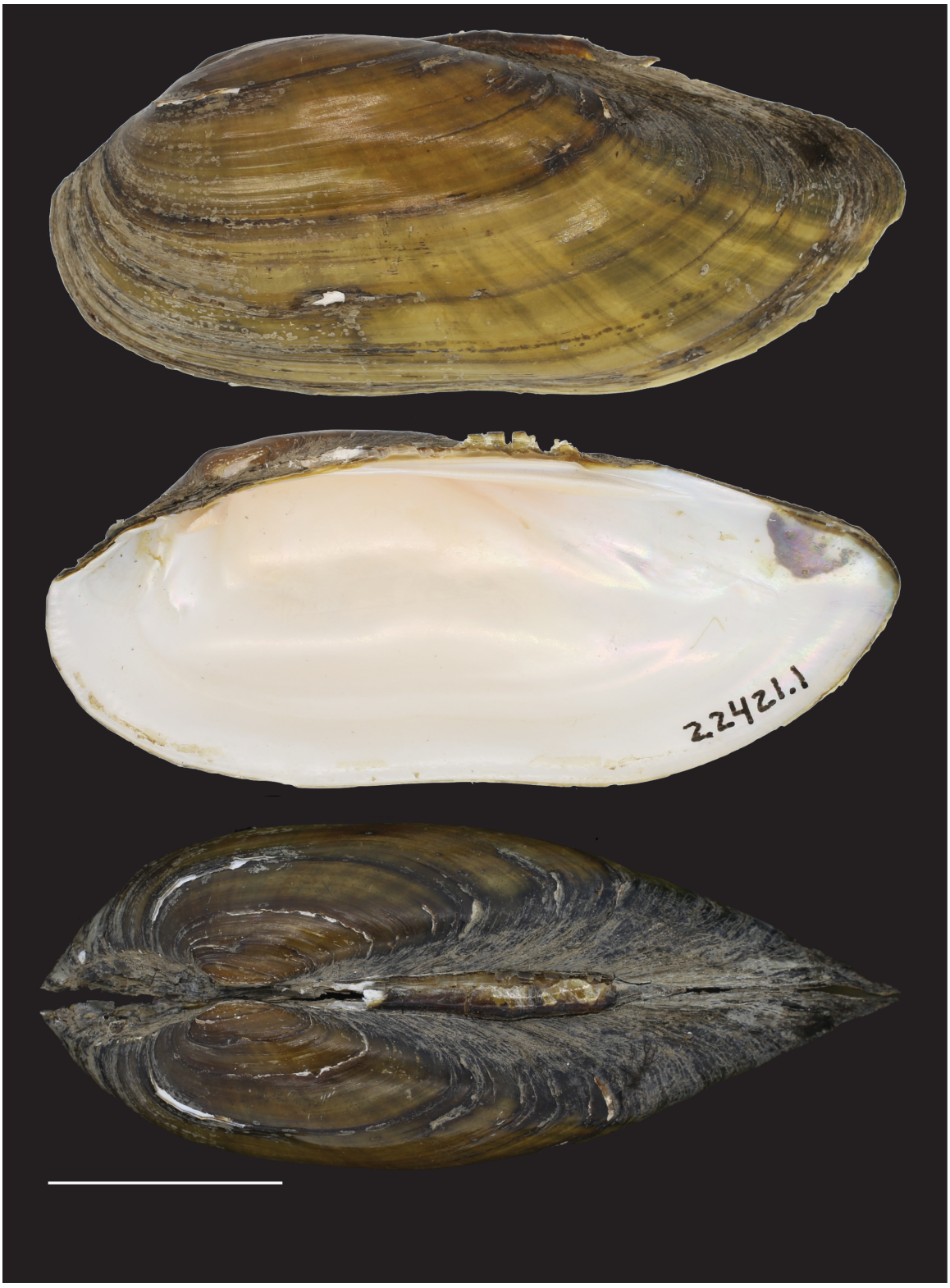

Figure 1.12. *Lampsilis teres* neotype JFBM 22421.1. Scale bar is 30mm.

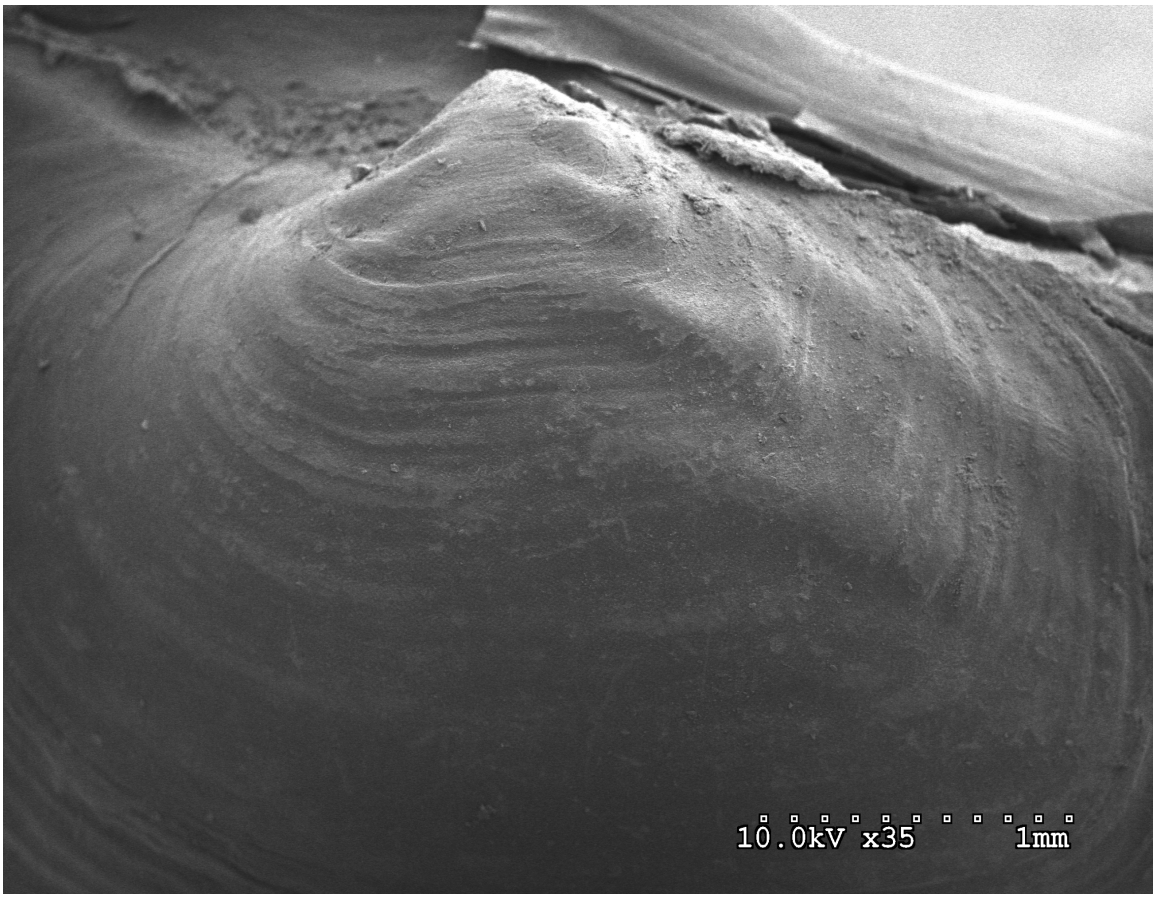

Figure 1.13. Beak sculpture of *L. anodontoides* JFBM 22438.5.

Figure 1.14. *Lampsilis anodontoides* neotype JFBM 22433. Scale bar is 30mm.

BIBLIOGRAPHY

Adams, D. C., M. L. Collyer, and A. Kaliontzopoulou. 2018. Geomorph: Software for geometric morphometric analyses. R package version 3.0.6.

Baker, F.C. 1898. *The mollusca of the Chicago area.* The Academy.

Baker, F.C. 1928. Fresh Water Mollusca of Wisconsin.

Bouckaert, R., J. Heled, D. Kühnert, T. Vaughan, C.H. Wu, D. Xie, M.A. Suchard, A. Rambaut, and A.J. Drummond. 2014. BEAST 2: a software platform for Bayesian evolutionary analysis. PLoS computational biology. 10.

Buhay, J.E., J.M. Serb, C.R. Dean, Q. Parham, and C., Lydeard. 2002. Conservation genetics of two endangered unionid bivalve species, *Epioblasma florentina walkeri* and *E. capsaeformis* (Unionidae: Lampsilini). Journal of Molluscan Studies. 68: 385-391.

Burdick, R.C. and M.M. White, 2007. Phylogeography of the wabash pigtoe, *Fusconaia flava* (Rafinesque, 1820) (Bivalvia: Unionidae). Journal of Molluscan Studies. 73: 367-375.

Call, R.E. 1900. A descriptive catalogue of the Mollusca of Indiana. Rept. Indiana Dept. Geol. Nat. Res. 335-353.

Carstens, B.C., T.A. Pelletier, N.M. Reid, and J.D. Satler. 2013. How to fail at species delimitation. Molecular ecology. 22: 4369-4383.

Campbell, D.C., J.M. Serb, J.E. Buhay, K.J. Roe, R.L. Minton, and C. Lydeard. 2005. Phylogeny of North American amblemines (Bivalvia, Unionoida): prodigious polyphyly proves pervasive across genera. Invertebrate Biology. 124: 131-164.

Conrad, T.A., 1836. Monography of the Unionidae, or Naiades of Lamarck.

Clement, M., Q. Snell, P. Walke, D. Posada, K. Crandall. 2002. TCS: estimating gene genealogies. Proc. 16th Int. Parallel Distrib. Process Symp. 2: 184.

Curran, J. 2017. Hotelling's T^2 Test and Variants.

De Queiroz, K., 2007. Species concepts and species delimitation. Systematic biology. 56: 879-886.

Edgar, R.C., 2004. MUSCLE: a multiple sequence alignment method with reduced time and space complexity. BMC bioinformatics. 5:113.

Elderkin, C.L., A.D. Christian, C.C. Vaughn, J.L. Metcalfe-Smith, and D.J. Berg. 2007. Population genetics of the freshwater mussel, *Amblema plicata* (Say 1817) (Bivalvia: Unionidae): evidence of high dispersal and post-glacial colonization. Conservation Genetics. 8: 355-372.

Elderkin, C.L., A.D. Christian, J.L. Metcalfe-Smith, and D.J. Berg. 2008. Population genetics and phylogeography of freshwater mussels in North America, *Elliptio dilatata* and *Actinonaias ligamentina* (Bivalvia: Unionidae). Molecular ecology. 17: 2149.

Folmer, O., M. Black, W. Hoeh, R. Lutz, and R. Vrijenhoek. 1994. DNA primers for amplification of mitochondrial cytochrome c oxidase subunit I from diverse metazoan invertebrates. Molecular marine biology and biotechnology. 3: 294-299.

Fujita, M.K., A.D. Leaché, F.T. Burbrink, J.A. McGuire, and C. Moritz. 2012. Coalescent-based species delimitation in an integrative taxonomy. Trends in ecology & evolution. 27: 480-488.

Freshwater Mollusk Conservation Society. 2016. A national strategy for the conservation of native freshwater mollusks. Freshwater Mollusk Biology and Conservation. 19: 1–21.

Graf, D.L. and K.S. Cummings. 2018. The Freshwater Mussels (Unionoida) of the World (and other less consequential bivalves), updated 30 March 2018. MUSSEL Project Web Site. http://www.mussel-project.net/.

Graf, D.L. and D.Ó. Foighil. 2000. The evolution of brooding characters among the freshwater pearly mussels (Bivalvia: Unionoidea) of North America. Journal of Molluscan Studies. 66: 157-170.

Haag, W.R. 2010. A hierarchical classification of freshwater mussel diversity in North America. Journal of Biogeography. 37: 12-26.

Haag, W.R. 2012. *North American freshwater mussels: natural history, ecology, and conservation*. Cambridge University Press.

Haag, W.R. and J.D. Williams. 2014. Biodiversity on the brink: an assessment of conservation strategies for North American freshwater mussels. Hydrobiologia. 735: 45-60.

Hanley, S. 1842. An illustrated and descriptive catalogue of recent bivalve shells.

Harris, J.L., W.R. Hoeh, A.D. Christian, J.L. Walker, J.L. Farris, R.L. Johnson, and M.E. Gordon. 2004. Species limits and phylogeography of Lampsilinae (Bivalvia; Unionoida) in Arkansas with emphasis on species of *Lampsilis*. Unpublished final

report to Arkansas Game and Fish Commission and US Fish and Wildlife Service. 70.

Hershler, R., H.P. Liu, and C. Bradford. 2013. Systematics of a widely distributed western North American springsnail, Pyrgulopsis micrococcus (Caenogastropoda, Hydrobiidae), with descriptions of three new congeners. ZooKeys. 330: 27.

Hess, M.C., K. Inoue, E.T. Tsakiris, M. Hart, J. Morton, J. Dudding, C.R. Robertson, and C.R. Randklev. 2018. Misidentification of sex for *Lampsilis teres*, Yellow Sandshell, and its implications for mussel conservation and wildlife management. PloS one. 13.

Inoue, K., D.M. Hayes, J.L. Harris, and A.D. Christian. 2013. Phylogenetic and morphometric analyses reveal ecophenotypic plasticity in freshwater mussels *Obovaria jacksoniana* and *Villosa arkansasensis* (Bivalvia: Unionidae). Ecology and Evolution. 3: 2670-2683.

Inoue, K., D.M. Hayes, J.L. Harris, N.A. Johnson, C.L. Morrison, M.S. Eackles, T.L. King, J.W. Jones, E.M. Hallerman, A.D. Christian, and C.R. Randklev. 2018. The Pleurobemini (Bivalvia: Unionida) revisited: molecular species delineation using a mitochondrial DNA gene reveals multiple conspecifics and undescribed species. Invertebrate Systematics. 32: 689-702.

King, T.L., M.S. Eackles, B. Gjetvaj, and W.R. Hoeh. 1999. Intraspecific phylogeography of *Lasmigona subviridis* (Bivalvia: Unionidae): conservation implications of range discontinuity. Molecular Ecology. 8.

Kuehnl, K.F., 2009. Exploring levels of genetic variation in the freshwater mussel genus *Villosa* (Bivalvia Unionidae) at different spatial and systematic scales: implications for biogeography, taxonomy, and conservation. The Ohio State University.

Kumar, S., G. Stecher, and K. Tamura. 2016. MEGA7: molecular evolutionary genetics analysis version 7.0 for bigger datasets. Molecular biology and evolution. 33: 1870-1874.

Lanfear, R., B. Calcott, S.Y. Ho, and S. Guindon. 2012. PartitionFinder: combined selection of partitioning schemes and substitution models for phylogenetic analyses. Molecular biology and evolution. 29: 1695-1701.

Lea, I. 1831. Observations on the naiades, and descriptions of new species of that and other families. Transactions of the American Philosophical Society. 4: 63-121.

Lea, I. 1852. *A Synopsis of the Family Naiades*. Blanchard and Lea.

Leigh, J.W. and D. Bryant 2015. PopART: Full-feature software for haplotype network construction. Methods Ecol. Evol .6: 1110–1116.

Mathiak, H.A. 1979. *A river survey of the unionid mussels of Wisconsin, 1973-1977*. Sand Shell Press.

Meyer, D. and F.T. Wien. 2001. Support vector machines. R News. 1: 23-26.

Miller, M.A., W. Pfeiffer, and T. Schwartz. 2010. Creating the CIPRES Science Gateway for inference of large phylogenetic trees. Gateway Computing Environments Workshop (GCE).

Mulvey, M., C. Lydeard, D.L. Pyer, K.M. Hicks, J. Brim-Box, J.D. Williams, and R.S. Butler. 1997. Conservation genetics of North American freshwater mussels *Amblema* and *Megalonaias*. Conservation Biology. 11: 868-878.

Murray, H.D. and A.B. Leonard. 1962. *Handbook of unionid mussels in Kansas*. Museum of Natural History University of Kansas.

Oesch, R.D. 1984. *Missouri naiades: a guide to the mussels of Missouri*. Missouri Department of Conservation.

Parmalee, P.W. and A.E. Bogan. 1998. *Freshwater mussels of Tennessee*. University of Tennessee Press.

Pfeiffer, J.M., N.A. Johnson, C.R. Randklev, R.G. Howells, and J.D. Williams. 2016. Generic reclassification and species boundaries in the rediscovered freshwater mussel '*Quadrula*'*mitchelli* (Simpson in Dall, 1896). Conservation genetics. 17: 279-292.

Pfeiffer, J.M., A.E. Sharpe, N.A. Johnson, K.F. Emery, and L.M. Page. 2018. Molecular phylogeny of the Nearctic and Mesoamerican freshwater mussel genus *Megalonaias*. Hydrobiologia. 811: 139-151.

Pfenninger, M., S. Staubach, C. Albrecht, B. Streit, and K. Schwenk. 2003. Ecological and morphological differentiation among cryptic evolutionary lineages in freshwater limpets of the nominal form-group *Ancylus fluviatilis* (OF Müller, 1774). Molecular Ecology. 12: 2731-2745.

Pieri, A.M., K. Inoue, N.A. Johnson, C.H. Smith, J.L. Harris, C. Robertson, and C.R. Randklev. 2018. Molecular and morphometric analyses reveal cryptic diversity within freshwater mussels (Bivalvia: Unionidae) of the western Gulf coastal drainages of the USA. Biological Journal of the Linnean Society, 124: 261-277.

R Core Team 2013. R: A language and environment for statistical computing. R Foundation for Statistical Computing, Vienna, Austria.

Rafinesque, C.S. 1820. Monographie des coquilles bivalves fluviatiles de la Riviere Ohio, contenant douze genres et soixante-huit especes. Annales generales des sciences Physiques, a Bruxelles. 5: 287-322.

Rambaut, A., M.A. Suchard, D. Xie, and A.J. Drummond. 2014. Tracer v1. 6. Computer program and documentation distributed by the author.

Simpson, C.T. 1914. *A descriptive catalogue of the naiades. or pearly freshwater mussels.* Bryant Walker, Detroit.

Smith, C.H., N.A. Johnson, J.M. Pfeiffer, and M.M. Gangloff. 2018. Molecular and morphological data reveal non-monophyly and speciation in imperiled freshwater mussels (*Anodontoides* and *Strophitus*). Molecular phylogenetics and evolution. 119: 50-62.

Smith, H.M. 1899. *The mussel fishery and pearl-button industry of the Mississippi River*. US Government Printing Office.

Stamatakis, A. 2014. RAxML version 8: a tool for phylogenetic analysis and post-analysis of large phylogenies. Bioinformatics. 30: 1312-1313.

Therneau, T., B. Atkinson, B. Ripley, and M.B. Ripley. 2018. Package 'rpart'.

Turgeon, D.D., A.E. Bogan, E.V. Coan, W.K. Emerson, W.G. Lyons, W.L. Pratt, C.F.E. Roper, A. Scheltema, E.G. Thompson, and J.D. Williams. 1988. Common and Scientific Names of Aquatic Invertebrates from the United States and Canada: Mollusks. American Malacological Union. American Fisheries Society Special Publication, 16.

Utterback, W.I. 1916. *The naiades of Missouri*. University Press.

Wang, H., L. He, X. Yang, S. Yang, C. Li, and X. Wang. 2016. Determination of the complete mitochondrial genome sequence of mussel *Cristaria plicata* (Leach). Mitochondrial DNA Part A. 27: 1478-1479.

Watters, G.T., M.A. Hoggarth, and D.H. Stansberry. 2009. *The freshwater mussels of Ohio*. The Ohio State University Press.

Wickham, H. 2009. ggplot2: Elegant Graphics for Data Analysis. Springer-Verlag New York.

Williams, J.D., M.L. Warren Jr, K.S. Cummings, J.L. Harris, and R.J. Neves. 1993. Conservation status of freshwater mussels of the United States and Canada. Fisheries. 18: 6-22.

Williams, J.D., A.E Bogan, and J.T. Garner. 2008. *Freshwater mussels of Alabama and the Mobile basin in Georgia, Mississippi, and Tennessee*. University of Alabama Press.

Williams, J.D., A.E. Bogan, R.S. Butler, K.S. Cummings, J.T. Garner, J.L. Harris, N.A Johnson, and G.T. Watters. 2017. A revised list of the freshwater mussels (Mollusca: Bivalvia: Unionida) of the United States and Canada. Freshwater Mollusk Biology and Conservation. 20: 33-58.